THE ASTROPHYSICAL JOURNAL, 448:521–547, 1995 August 1

ON THE FR I/FR II DICHOTOMY IN POWERFUL RADIO SOURCES: ANALYSIS OF THEIR EMISSION-LINE AND RADIO LUMINOSITIES

ESTHER L. ZIRBEL AND STEFI A. BAUM
Space Telescope Science Institute,[1] 3700 San Martin Drive, Baltimore, MD 21218
Received 1994 August 5; accepted 1995 February 7

ABSTRACT

We know from previous work that there are substantial differences between powerful FR I and FR II radio galaxies. In this paper we look at the correlations of line luminosity, radio luminosity, core radio power, and host galaxy optical magnitude independently for FR I and FR II radio galaxies and compare these correlations with those for an optically selected control sample of early-type galaxies. In this, Paper I in a two-paper series, we list the principal results; in Paper II we discuss the implications of these results for our understanding of the FR I–FR II dichotomy and the central engines of powerful radio galaxies.

Our principal results are the following. Correlating core power to total power we find: (1) The difference between the radio core powers of FR I and FR II galaxies is less than the difference between the extended radio powers: the median total radio powers of FR II galaxies in our sample are about 40 times greater than those of FR I galaxies, while the median radio core powers of FR II galaxies in our sample are only about 4 times greater than those of FR I galaxies. (2) In agreement with previous work, we find a decrease (with slope -0.38 ± 0.05) in the ratio of core to lobe radio power, the *R*-parameter, with increasing total radio power. However, there is a significant scatter (2 orders of magnitude) in the *R*-parameter. (3) At a fixed total radio power, FR I and FR II galaxies have the same ratio of core to lobe power and a comparable scatter.

We investigate the possibility of systematic effects skewing these results but find no evidence for this: (1) The *R*-parameter is not affected by redshift selection effects. (2) Orientation and beaming effects are either dominated by the large intrinsic scatter in the *R*-parameter, or they themselves produce that scatter. Since the scatter is the same for FR I and FR II sources, beaming effects must be equally important or unimportant in both FR types.

We analyze the three-way correlation between redshift, radio power, and emission-line luminosity and find that the correlation of radio power with redshift is stronger than that of emission-line luminosity with redshift. In fact, for the FR I galaxies there is virtually no correlation between line luminosity and redshift.

When correlating the total radio power to the emission-line luminosity for our full sample of radio-loud galaxies, we find that these two parameters are strongly correlated over 8 orders of magnitude in emission-line luminosity and 10 orders of magnitude in total radio power. When we look independently at the correlations for FR I and FR II radio galaxies, we find: (1) Each FR type has its own independent correlation of radio power and emission-line luminosity. (2) The functional relationships between emission-line luminosity ($L_{\rm line}$) and radio power ($P_{408\,\rm MHz}$) are different; $L_{\rm line} = (0.75 \pm 0.08) \times P_{408\,\rm MHz} + (14.8 \pm 2.3)$ for FR II galaxies and $L_{\rm line} = (0.28 \pm 0.07) \times P_{408\,\rm MHz} + (26.3 \pm 1.8)$ for FR I galaxies. (3) The FR I and FR II radio sources are offset with respect to one another in the radio-line luminosity plane, which can be described in two fashions: for the same total radio power as the FR I galaxies, the FR II galaxies produce consistently about 5–30 times as much emission-line luminosity; or, for the same amount of emission-line activity as the FR II galaxies, the FR I galaxies produce about 10–100 times as much total radio power. (4) For FR I sources and optically selected sources, we find a correlation of line luminosity with host galaxy optical magnitude (there is none for FR II galaxies). Removing the dependence of line luminosity on host galaxy optical magnitude, we find a 2 σ dependence of line luminosity on radio luminosity for FR I sources.

Correlating the core radio powers to the emission-line luminosities, we find: (1) Each FR type has its own correlation between the radio core power and the emission-line luminosity. Both correlations are as good as those between total power and emission-line luminosity. (2) The functional relationships for FR I and FR II sources are again different; $L_{\rm line} = (0.62 \pm 0.10) \times P_{\rm core} + (19.9 \pm 2.3)$ for FR II galaxies and $L_{\rm line} = (0.30 \pm 0.12) \times P_{\rm core} + (26.3 \pm 2.8)$ for FR I galaxies. (3) The two FR types separate out even more clearly in the core radio power–emission-line luminosity plane than in the total radio power–line luminosity plane. For the same radio core power as the FR I galaxies, the FR II galaxies produce consistently about 10–50 times as much emission-line luminosity; or, for the same amount of emission-line activity as the FR II galaxies, the FR I galaxies produce about 200–300 times as much radio core power.

The most important result is that FR I and FR II radio sources display strong differences in their correlations of line luminosity, ratio total and core power, and host galaxy optical magnitude. These differences may reflect fundamental differences in the properties of the central engines in these two types of radio galaxies. A detailed discussion of the implications is deferred to Paper II.

Subject headings: galaxies: fundamental parameters — radio continuum: galaxies

[1] Operated by the Association of Universities for Research in Astronomy, Inc., under contract with the National Aeronautics and Space Administration.

1. INTRODUCTION

It was 20 years ago that Fanaroff & Riley (1974) first noted the dichotomy between the radio appearance of high- and low-power radio galaxies with extended, double-lobed radio structure. In gross terms, they classified them into two groups: the Fanaroff & Riley Class I (FR I) and Class II (FR II) radio galaxies. In the FR I radio galaxies, the radio emission peaks near the center of the galaxy and the twin jets fade with distance from the center producing the diffuse, plumelike and "edge-dimmed" radio lobes. On the other hand, the FR II radio galaxies have "edge-brightened" radio lobes which possess small-scale high surface brightness regions ("hot spots") that are filled by invisible or predominantly one-sided jets.[2] The remarkable result of Fanaroff & Riley (1974) is that the radio morphology strongly correlates with radio power: radio sources with radio powers of less than 10^{25} W Hz^{-1} at 408 MHz show almost exclusively FR I morphologies while the higher power sources with radio powers larger than 10^{27} W Hz^{-1} show almost exclusively FR II morphologies. At radio powers ranging from $P_{408\,\mathrm{MHz}} = 10^{25}$–$10^{27}$ W Hz^{-1} there is a considerable "overlap" over which FR I and FR II radio galaxies coexist in roughly equal numbers. In this "overlap region," many sources can be identified as either an FR I or an FR II; however, sources with intermediate (or indeterminate) radio morphologies also exist (e.g., Baum et al. 1988; Owen & Laing 1989; Morganti, Killeen, & Tadhunter 1993; Capetti, Parma, & Fanti 1994).

Since 1974, much progress has been made on the study of the distinctions between the properties of the FR I and FR II radio galaxies. We know now that the dichotomy between these two classes encompasses much beyond their radio appearances, including the nature of their host galaxies (e.g., Smith 1988; Allington-Smith et al. 1993; Zirbel 1994a; Heckman et al. 1986; Owen & Laing 1989; Owen & White 1991), kinematics within their host galaxies (e.g., Smith, Heckman, & Illingworth 1990; Baum, Heckman, & van Breugel 1992), their host galaxy environments (e.g., Prestage & Peacock 1988; Yates, Miller, & Peacock 1989; Hill & Lilly 1989; Allington-Smith et al. 1993; Zirbel 1994b), their far-IR properties (e.g., Heckman et al. 1994) and their optical emission lines (e.g., Longair & Riley 1979; Baum & Heckman 1989a, b; Caganoff 1988; McCarthy 1988; Rawlings et al. 1989; Saunders et al. 1989; Morganti, Ulrich, & Tadhunter 1992; Rawlings & Saunders 1992; Morganti et al. 1993).

In this paper, we seek to address the question of the differences seen between the FR I's and the FR II's by investigating the correlations between total radio power, core radio power, emission-line luminosity, and host galaxy optical magnitude for a large sample of radio galaxies (taken from the literature). This work complements many earlier studies of optical line and radio luminosity which had found a strong empirical link between the narrow emission-line luminosity and the total radio power spanning over four orders of magnitude in both parameters (see above references). However, many of these studies which show a strong correlation of radio to line luminosity were dominated by samples of high-luminosity radio galaxies (i.e., mostly FR II sources), while similar studies of the line to radio luminosity correlation in lower luminosity samples showed mixed results (e.g., Morganti et al. 1992, who find a correlation which is somewhat flatter than that for more powerful radio sources, and Caganoff 1989, who found no correlation). Our sample spans 10 orders of magnitude in radio luminosity, and more importantly it contains a large number of FR I and FR II sources which overlap in radio luminosity. Thus, we can use this sample to determine which properties correlate with radio luminosity and which correlate with Fanaroff and Riley type (i.e., we can disentangle the importance of radio luminosity from radio morphology).

The outline of this paper is as follows. In § 2 we describe our sample and how we have compiled the necessary data from the literature. In § 3, we present the results. We start by discussing redshift selection effects that may contaminate any of the correlations in this paper. The first correlation that we analyze is that between total radio power and core radio power. Following that, we analyze the correlations of emission-line luminosity with total radio power and with core radio power and with the optical magnitude of the host galaxy. We show that the correlations of emission-line luminosity with total radio power, core radio power, and optical magnitude are indeed different for the FR I's and the FR II's. On the other hand, we show that at a fixed total radio power the FR I's and the FR II's have the same ratio of core to total radio power. In § 4 we summarize the principal results. The interpretation of the results is left to Paper II.

2. THE SAMPLE

We have put together the largest sample of radio-loud elliptical galaxies (excluding quasars) from the literature for which we could accumulate reliable emission-line and radio luminosities. We obtain the data for the radio sources from Baum & Heckman (1989a, b), Caganoff (1988), McCarthy (1988), Giovannini et al. (1988), Morganti et al. (1992, 1993), Tadhunter et al. (1993), Rawlings et al. (1989), Rawlings & Saunders (1992), Sadler, Jenkins, & Kotanyi (1989), Benn et al. (1993), Rowan-Robinson et al. (1993), and Allington-Smith et al. (1993). We have created a "control" sample of optically selected early-type galaxies with which to compare our results for the radio galaxies. This control sample is composed of early-type galaxies taken from Phillips et al. (1986) and Goudfrooij et al. (1993, 1994). The final list of radio galaxies can be found in the Appendix.

The approach of putting together a sample from the listed references has two principal risks: (1) We are mixing data taken from different samples taken with different instruments, at different wavelengths, and with different resolutions and levels of accuracy. Thus we may "lose" information in the extra measurement noise or incorrectly find effects which are due to measurement differences which we attribute to real structural differences in the sources. (2) Since the sample is not a "complete" sample in any way, selection effects may enter which may influence our conclusions. Both "dangers" are addressed below. Despite the risks, the benefits of compiling a sample in this way are clear.

Our sample consists of total radio powers measured at 408 MHz, radio core powers measured at 5 GHz, emission-line luminosities measured in Hα + [N II], and absolute V magnitudes. The details of compiling the input data and converting them to the same scales are described in detail below. We chose units of watts per hertz (W Hz^{-1}) for the radio powers and watts (W) for the emission-line luminosities. We adopt $H_0 = 50$ km s^{-1} Mpc^{-1} and $q_0 = 0.0$ throughout.

[2] For a more detailed review of the radio properties of FR I and FR II sources, the reader is referred to Bridle & Perley (1984); Bridle (1992); McCarthy (1993); or Laing (1993).

The final sample spans over 10 orders of magnitude in line and radio luminosity ranging from the "radio-quiet" ellipticals of Phillips et al. (1986) to the more powerful radio galaxies of McCarthy (1988). This nicely covers FR I and FR II radio galaxies which are located within the "transition region" in radio power. However, one drawback of our sample is that it does not include positively identified FR I sources that are fainter than 10^{24} W Hz^{-1} (these are analyzed by Owen, Ledlow, & Keel 1994). Nevertheless, this sample is still well suited for searching for systematic differences between the two fundamental classes of radio galaxies and for isolating the influence of radio luminosity on source properties.

2.1. *The Radio Morphology Classification*

We take the FR classifications of the sources as listed in the appropriate papers. The only exemptions are Caganoff's sources, which we chose to reclassify from the original radio maps because we noted some inconsistencies. One general problem with the FR scheme is that the radio morphology of some sources may be rather complex. Therefore, it is not surprising that there are discrepancies in the literature in the radio morphology classification. Some examples are 3C 17, 3C 277.3, 3C 433, 3C 196.1, and 3C 452, which were identified as FR I's by Laing, Riley, & Longair (1983) and by Yates et al. (1989) and as FR II's by Prestage & Peacock (1988). Baum & Heckman (1989a, b) partially avoid this problem by classifying 3C 433 and 3C 196.1 as amorphous. While the original FR classification scheme is quantitative, in practice it depends (1) on what each researcher calls edge darkened and edge brightened and (2) on the frequency and the resolution of the radio map used to perform the classification. The main point is that the "applied" FR scheme is not only subjective, but also that mixed breeds do exist (e.g., Baum et al. 1988; Morganti et al. 1993; Capetti et al. 1994). This can be seen in detailed radio maps of sources that exhibit both FR I and FR II properties simultaneously. For example, Capetti et al. (1994) present sources which have narrow jets with distinct hot spots, which are characteristic of FR II sources, but which diffuse at larger distances and thus produce edge-darkened lobes, which are characteristic of FR I sources. Since the purpose of this paper is to compare the "classical" FR I to the "classical" FR II sources, we decided that whenever we encounter discrepancies in the FR classification, we shall include them only when specifically noted. We exclude unresolved sources and sources which have a nonextended structure.

Our sample includes some high-redshift sources ($0.5 < z < 1.5$). Since most of those sources have radio powers (with $P_{408\,\mathrm{MHz}} > 10^{27}$ W Hz^{-1}) which are well above the break in the radio luminosity function, it is likely that the majority are FR II sources. However, it is uncertain if the emission-line properties of these sources are comparable to their lower redshift counterparts. For example, studies of high-redshift radio galaxies have shown that their emission-line regions may be very extended and that the alignment between the radio axis and the emission-line regions can be very strong (e.g., McCarthy et al. 1987; Chambers, Miley, & van Breugel 1987). Therefore, we use a different symbol to denote the $z > 0.5$ sources, and we consider the correlations we derive with and without them.

On the other hand, since the lower power sources of Phillips et al. (1986) or Sadler et al. (1989) have total radio powers which are well below the break in the radio luminosity function, they are likely to be either FR I sources or unresolved nuclear sources. Nevertheless, we shall consider them separately from positively identified FR I sources and assign different symbols to them.

2.2. *Total Radio Powers and Radio Core Powers*

We chose to evaluate the total radio powers at a frequency of 408 MHz to minimize the potential impact of beaming; 408 MHz is the lowest frequency at which we have reliable fluxes for the majority of the sources. For sources in which no 408 MHz flux was available, we converted the measured flux adopting the lowest frequency spectral index available; for sources with no reliable spectral index measurement, we adopt $\alpha = 0.75$, where $S_\nu \propto \nu^{-\alpha}$ to convert the flux to 408 MHz.

The radio core fluxes of the sources in our sample are all calculated at a frequency of 5 GHz, mostly because this frequency was quoted in the majority of the references. Throughout this paper we shall therefore use $P_{\mathrm{tot}(408\,\mathrm{MHz})}$ and $P_{\mathrm{core}(5\,\mathrm{GHz})}$.

2.3. *The Emission-Line Luminosities*

We decided to analyze only the narrow emission-line fluxes, excluding all measurements of broad emission lines, i.e., for broad line radio galaxies (BLRG's) we only take their narrow emission-line fluxes. We decided to use the fluxes measured in Hα and [N II] λλ6584, 6548 combined, because these are quoted in the majority of the references. However, some sources, particularly at high redshift, were measured in [O II] λ3727 or in [O III] λ4959/λ5007. (For simplicity, we shall abbreviate [O III] λ4959/λ5007 as [O III], [O II] λ3727 as [O II], and Hα + [N II] λλ6584, 6548 as Hα throughout this paper.) We convert [O III] and [O II] to Hα fluxes by assuming the empirical correlations Hα/[O II] = 4.0 and Hα/[O III] = 1.1 (McCarthy 1988). Since McCarthy's calculations of the emission-line ratios were strongly dominated by FR II sources, and since we know from Heckman et al. (1989) and Baum et al. (1992) that emission-line ratios are very different for the FR I's and the FR II's, we need to evaluate these ratios for the FR I's. From Koski (1978) and Cohen & Osterbrock (1981) we obtain [O III] and Hα line luminosities for nine FR I's. Since Baum et al. (1992) find that FR I radio galaxies and cooling flow galaxies have comparable emission-line ratios, we also calculate this ratio for cooling flow galaxies from Johnstone, Fabian, & Nulsen (1987) and from Crawford, Fabian, & Johnstone (1987). In addition, among our combined sample we find seven more sources for which we have both [O III] and Hα emission-line luminosities. Altogether we have 21 FR I and cooling flow galaxies for which we calculate Hα/[O III] = 0.83 ± 0.34.

The emission-line luminosities of the galaxies in our sample have been calculated mostly from narrow-band imaging, although in some cases they were calculated from slit spectra. This is the case for Caganoff's radio sources and for the Phillips et al. ellipticals. Therefore, we need to check if their slit spectra emission-line luminosities are compatible with the remaining narrow-band imaging emission-line luminosities.

Baum & Heckman (1989b) analyzed the ratio of nuclear to extended emission-line fluxes for their sources and found that typically 90% of the line luminosity comes from within the inner 2.5 kpc of the nucleus, though individual sources in which the majority of the line luminosity comes from beyond this region do exist. Since typical errors on the photometry of the narrow-band emission-line imaging are of the order of 20%, errors introduced by using spectroscopy are typically within that scatter, though there may be individual sources in which long-slit spectra significantly underestimate the total line luminosity.

For radio-quiet galaxies, Goudfrooij et al. (1994) find that the emission-line regions are typically smaller than in radio galaxies (the diameter of the ionized gas is ~ 1 kpc), and they calculate the emission-line luminosities from both slit spectra and imaging and find no significant difference. Therefore, we are confident that all our emission-line luminosity measurements of radio-loud and radio-quiet galaxies are indeed compatible.

2.4. *The Optically Selected Comparison Sample*

Our "optically selected" comparison sample is compiled from a combination of papers from Phillips et al. (1986), Goudfrooij et al. (1993, 1994), Trinchieri & di Serego Alighieri (1991), Shields (1991), and Buson et al. (1993).

Although Sadler et al. (1989) measured radio luminosities for 42% of the Phillips et al. galaxies (with a flux limit of 0.8 mJy at 5 GHz), it is most important to note that these galaxies were not selected according to their radio luminosities. Their radio powers are relatively low and range from 10^{20}–10^{24} W Hz^{-1}. Note that although the Sadler et al. sample is a subset of the Phillips et al. sample, we shall refer to the Sadler et al. sample whenever we consider correlations of low-power radio galaxies and the Phillips et al. sample whenever we discuss properties of "radio-quiet" galaxies.

Our "radio-quiet" comparison sample also includes the Shapeley Ames Elliptical galaxies, whose colors and magnitudes were measured by Goudfrooij et al. (1993) and whose emission-line properties were analyzed by Goudfrooij et al. (1994). Goudfrooij et al. (1994) detect emission-line gas in 57% of their galaxies and dust (i.e., nonionized gas) in 41%, and they find that the dust and the ionized gas are consistent with being physically associated with each other. Among our "radio-quiet" comparison sample, we have also included some X-ray selected ellipticals from Trinchieri & di Serego Alighieri (1991), Shields (1991), and Buson et al. (1993). We label these galaxies with different symbols and consider them in our analysis only when specifically noted.

2.5. *Compiling the Final Sample*

Since our data are compiled from many papers, we sometimes have several measurements for one source. For simplicity we take straight means in the total radio powers, the radio core powers, and the emission-line luminosities. If any two measurements are more than one order of magnitude different, we ignore both measurements. If three measurements exist for one source and one measurement is more than one order of magnitude different from the other two, we take the mean of the remaining two measurements. We only consider Morganti et al.'s (1993) total radio powers which are measured at 5 GHz when no other radio fluxes at a lower frequency exist for the same source. However, we do use their total 5 GHz fluxes when evaluating the ratio of core to total power (i.e., the *R*-parameter). Also, we only use the emission-line luminosities derived from the [O III] fluxes if no Hα fluxes are available. The final list of radio sources is found in the Appendix.

We obtain the rest frame *V*-magnitudes from Allington-Smith et al. (1993), Sandage (1972a, b, 1973a, b), Laing et al. (1983), Smith & Heckman (1989), and Hill & Lilly (1991). These magnitudes should be accurate to within 0.03 of a magnitude. Other magnitudes are obtained from Giovannini et al. (1988), Feretti et al. (1986), and Phillips et al. (1986), but these are only expected to be accurate to within a tenth of a magnitude. For some of the remaining radio sources, we obtain absolute magnitudes from additional sources in the literature.

In this paper, we shall analyze the correlations of line luminosity, radio luminosity, core radio power, and host galaxy optical magnitude with the aid of the Astronomical Survival Analysis (ASURV), which has been kindly provided by Feigelson, Isobe, & LaValley (1992).

3. RESULTS

In this section we consider the interrelationships between the total radio power, the radio core power, the emission-line luminosity, and host galaxy absolute magnitude. Whenever possible, we shall compare these correlations to those of radio-quiet galaxies. Also, we shall discuss how redshift selection effects influence any of these correlations. In paper II (Baum, Zirbel, & O'Dea 1995) we shall then discuss the implications of the results presented here.

3.1. *Correlations with Redshift*

Since our sample is based predominantly on samples which were themselves radio flux density limited, there is a strong "artificial" radio power redshift correlation, which is discussed more extensively by Zirbel (1994a) and previously by Baum & Heckman (1989b). Since the radio luminosity function is steep, all radio catalogs are dominated by the intrinsically least luminous sources which are above the selection limit of the detector. As this threshold luminosity increases rapidly with redshift, it produces a strong radio power redshift correlation. This can be observed in Figure 1, where the bottom right side of the plot is incomplete, particularly at higher redshifts.

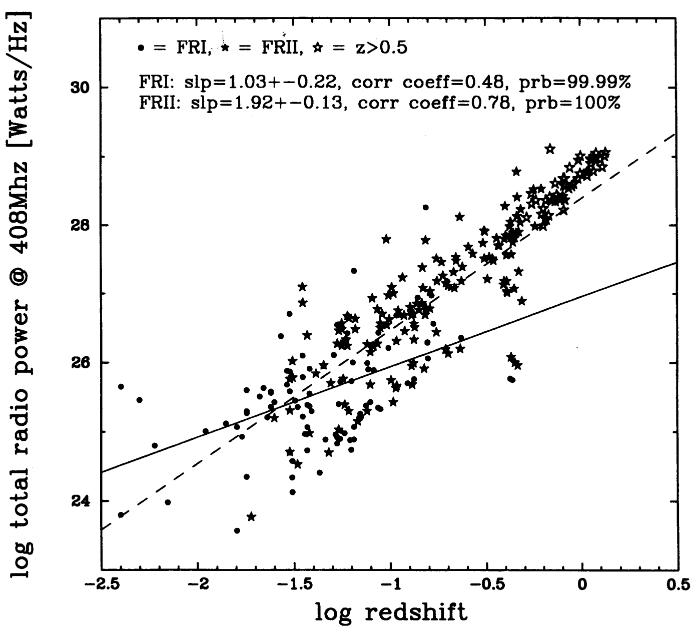

FIG. 1.—Logarithm of total radio power vs. logarithm of the redshift, separately for FR I and FR II sources. Using the subroutine SVDFIF from Press et al. (1992, p. 672), we obtain for the FR I's a slope of 1.03 ± 0.22, a *t*-statistic of 5.3, a correlation coefficient of 0.48, and a correlation probability of 99.99%. For the FR II's, corresponding values are 1.92 ± 0.13, 14.4, 0.78, and >99.99%.

TABLE 1

STATISTICS OF THE CORRELATION OF RADIO POWER WITH REDSHIFT AND EMISSION-LINE LUMINOSITY WITH REDSHIFT

	Radio Power		Line Luminosity	
Quantity	FR I	FR II	FR I	FR II
EM Algorithm				
Slope	1.03 ± 0.22	1.92 ± 0.13	0.47 ± 0.33	2.06 ± 0.22
Intersect	26.97 ± 0.32	28.38 ± 0.12	34.19 ± 0.50	36.82 ± 0.21
Standard deviation	0.77	0.57	0.83	0.75
Cox Correlation Hazard Model				
χ^2	15.82	140.73	0.74	52.76
Degrees of Freedom	1	1	1	1
Probability	99.99%	>99.99%	61%	>99.99%
Kendall's Tau Test				
z-value	3.699	10.455	1.165	7.294
Probability	99.98%	>99.99%	76	>99.99%

NOTES.—Statistics derived using ASURV. The redshift corresponds to the abscissa.

In Figure 1 we show the artificial radio power redshift correlation separately for the FR I and the FR II sources. We display the location of the higher redshift ($0.5 < z < 1.5$) FR II's and see that they are more strongly contaminated by redshift selection effects than their lower redshift counterparts. Note that in the sample presented in Figure 1, all powerful sources at high redshifts are FR II sources. Since it is important to analyze the properties of FR I and FR II sources over the same redshift range, we quote the statistics in Table 1 only for low-redshift sources, i.e., up to $z = 0.5$. Distinguishing between FR I's and FR II's, we see that the slopes are different, that of the FR II's being about twice that of the FR I's.

Since the intent of this paper is to analyze the correlation between radio and emission-line luminosity, this leaves us with a three-way correlation between radio power, redshift, and line luminosity which needs to be disentangled to prove unambiguously that there is a direct link between radio and line luminosity. Therefore, we need to compare the correlation of radio power with redshift to that of line luminosity with redshift.

In Figure 2 we show the correlation of emission-line luminosity with redshift separately for both FR types. We see immediately that the FR I's and the FR II's have different correlations. The statistics are listed in Table 1. Comparing the correlation probabilities and in particular the z-values of Kendall's Tau test of each FR type, we see that each of the correlations between radio power and redshift is stronger than that between line luminosity and redshift.

In Figure 2 of the line luminosity–redshift correlation, we see furthermore that the slopes of the FR I's and the FR II's are very different. Interestingly, the slope of the FR I's in the redshift versus line luminosity plot is virtually flat, suggesting that there is no or only marginal evolution in their emission-line luminosity.

3.2. *Correlations with Radio Power*

In this section, we examine the relationship between core and total radio power of FR I's and FR II's. We find that the ratio of core to extended radio power decreases with increasing radio luminosity which is consistent with previous work. However, contrary to previous belief, we find that the ratio of core to extended radio flux is the same for FR I's and FR II's of the same total radio luminosity.

3.2.1. *The Correlation of Total to Core Radio Power*

In Figure 3, we plot the total versus core radio powers for our entire sample of radio sources. At this stage, we do not differentiate between the two radio morphologies. We have marked the measurements from each group of researchers with a different symbol (this means that some sources may appear more than once in this plot). The purpose of showing this plot is twofold: to display the general location of the data from the different groups used in the analysis, and secondly, to show the

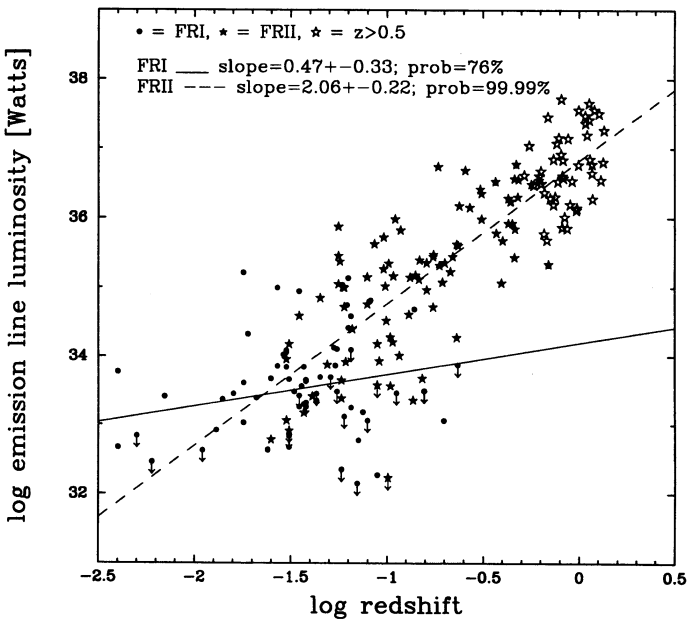

FIG. 2.—Logarithm of redshift vs. logarithm of the Hα + [N II] emission-line luminosity measured in watts, separately for FR I and FR II sources. Statistics of the fits are listed in Table 1 and are compared to the statistics of the fits of the correlation of the logarithm of the total radio power vs. the logarithm of the emission-line luminosity.

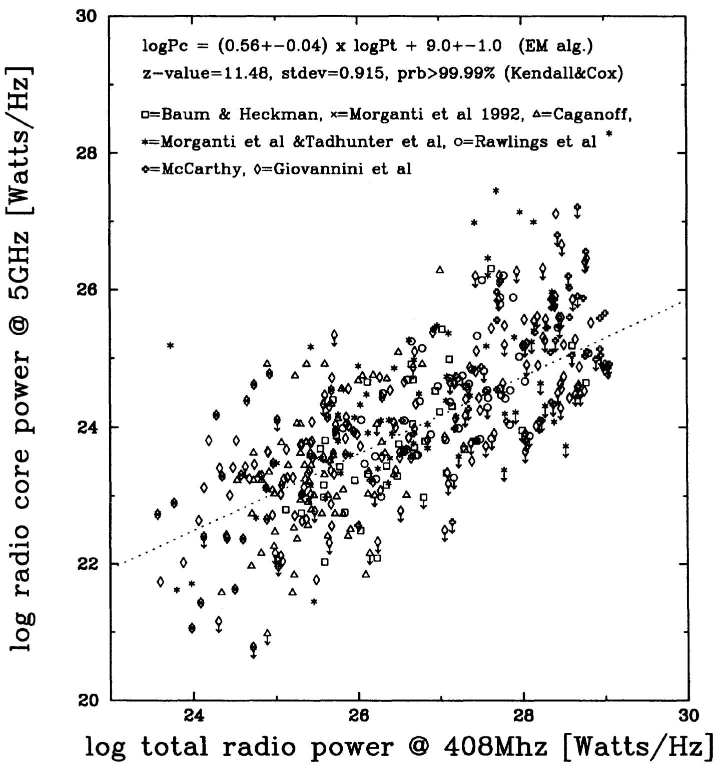

FIG. 3.—Logarithm of total radio power measured at 408 MHz in units of W Hz^{-1} vs. the logarithm of radio core power measured at 5 GHz, also in units of W Hz^{-1}. Each of the different groups that we use in our analysis is denoted by a different symbol. Note that some galaxies may appear more than once in this plot; however, the statistics of the line were calculated by replacing multiple measurements of each galaxy with one measurement.

overall trends. We see a strong correlation between core and total radio power spanning about seven orders of magnitude in both parameters.

In order to calculate the statistics for Figure 3, it is necessary to replace multiple measurements by one single measurement as outlined in § 2.5. Both the Kendall's Tau test and the Cox Correlation Hazard model (of Feigelson et al.'s ASURV) show that the correlation is significant at the 99.999% level. Using the fully parametric linear regression method (the EM algorithm, which stands for expectation and maximization), the best least-squares fit to the line is given by $\log P_{\rm core} = \log P_{\rm total} \times (0.56 \pm 0.04) + (9.0 \pm 1.0)$. The Buckley-James method gives very similar results. As noted in earlier works (Fabbiano et al. 1984); Giovannini et al. 1988; De Ruiter et al. 1990), the slope is not unity. However, we stress that the scatter is very large, i.e., 1 order of magnitude in both core and total radio power.

In Figures 4a and 4b, we plot the histograms of the logarithms of the total radio power and the radio core power separately for both FR types. Table 2 summarizes the means of the total and the radio core powers which were evaluated using the Kaplan-Meier Estimator, which treats data with upper and lower limits. A few points are immediately apparent: (1) The FR I's have both lower total radio powers (known since the original Fanaroff & Riley 1974 paper) and lower radio core powers than the FR II's. (2) There is a considerable overlap between the FR I's and the FR II's for total powers of $10^{25} < P_{408\,\rm MHz} < 10^{27}$ W Hz^{-1} and radio core powers of $10^{22} < P_{5\,\rm GHz} < 10^{26}$ W Hz^{-1} (i.e., there is a transition region in both the total radio power and the radio core power over which FR I and FR II radio galaxies "coexist" (also see Baum et al. 1988; Morganti et al. 1993). (3) The overlap in the radio core powers is larger than that in the total radio power. While the FR II's (including the $z > 0.5$ sources) in our sample have a median total radio power which is about 40 times greater than the median total radio power of the FR I's, the median core powers of the FR II's are only about 4 times greater than the median core powers of the FR I's.

3.2.2. *The Ratio of Core to Extended Radio Power*

To further explore the significance of the differences between the core and total radio power of FR I's and FR II's, we have evaluated the ratio of the radio core to radio lobe power for our sample. In the literature, this ratio is often referred to as the *R*-parameter (e.g., Giovannini et al. 1988; Feretti et al. 1984; Fabbiano et al. 1984; Fanti et al. 1987; De Ruiter et al. 1990), or as the orientation parameter (e.g., Padovani & Urry 1992). Orientation effects will be discussed in more detail in § 3.2.3.1. We calculate the ratio of core to lobe radio powers (or fluxes, *S*) via:

$$R = \frac{S_{\rm core(5\,GHz)}}{S_{\rm total_{freq}} \times (5\,{\rm GHz/freq})^{-\alpha} - S_{\rm core(5\,GHz)}} .$$

Ideally the *R*-parameter should be calculated from core and total fluxes that were obtained at the same frequency. Within our sample, this is the case only for the Morganti et al. (1993) data. All other *R*-parameters were calculated using the above formula, where "freq" is the frequency at which the total

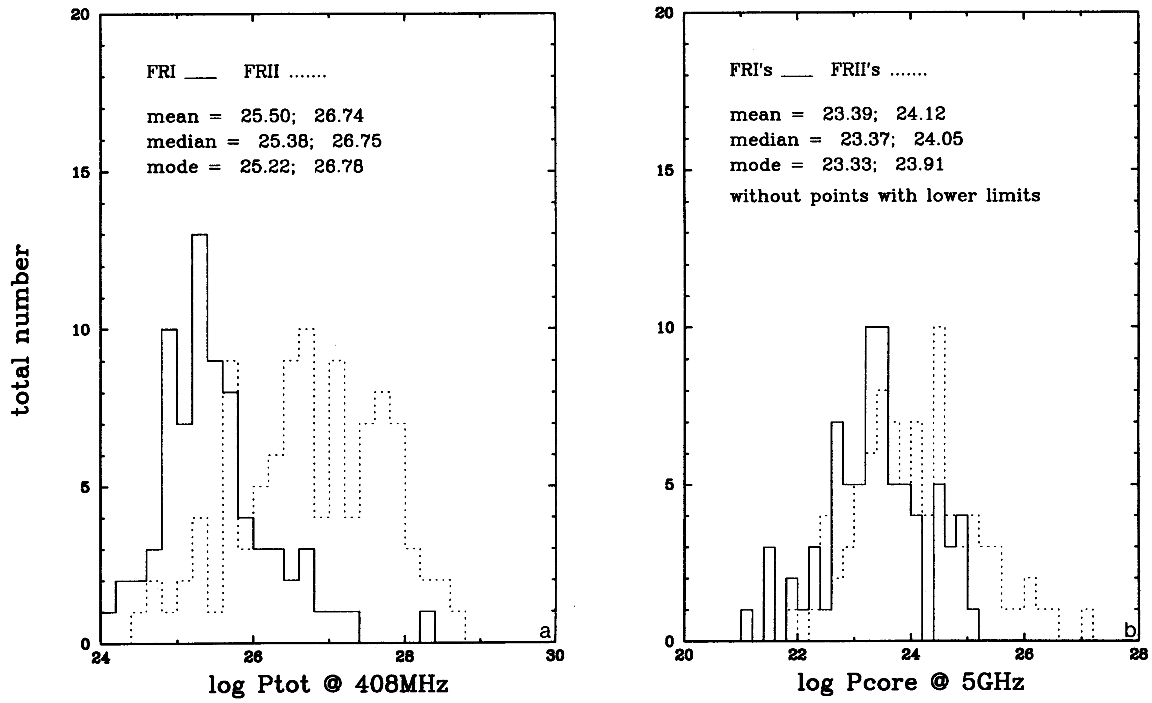

FIG. 4.—Histograms comparing (*a*) total radio power and (*b*) radio core powers of FR I's and FR II's. Fig. 2*b* contains some data which have upper limits which were treated as real detections in this plot. However, when using the Kaplan-Meier Estimator, we find that the means of the radio core powers of the FR I's are 23.33 ± 0.11, and those of the FR II's are 23.97 ± 0.11.

power was measured and α is the spectral index measured between "freq" and 5 GHz. In cases in which we do not have $\alpha_{5000}^{\rm freq}$, we adopted α_{2700}^{408} α_{1400}^{408} or even α_{1400}^{178} because the spectral index does not seem extremely variable over those wavelength regions. In cases in which no measurements of the spectral index exist, we adopted a mean of 0.75. This means that for sources with a low spectral index, the *R*-parameter will be overestimated. Nevertheless, we show later (§ 3.2.3.1) that these errors are minimal because differences in the *R*-parameter of different groups are insignificant. Also, note that the *R*-parameters are not affected by redshift selection effects (§ 3.2.3.2).

In Figure 5 we show the histograms of the *R*-parameters for the FR I's and the FR II's. Again, there is a definite region of overlap for $-2.0 < \log R < -1.0$, but on average the FR II's have higher *R*-parameters. Using the Kaplan-Meier Estimator, the mean *R*-parameters for the FR I's, the low-redshift FR II's, and the low- and high-redshift FR II's are $\langle \log R \rangle = -1.40 \pm 0.10$, -1.94 ± 0.11, and -2.20 ± 0.11, respectively. We conclude that the median value of the core to extended radio power is about 3–4 times higher in the FR I's than the FR II's in our sample.

In Figure 6 we plot the *R*-parameter versus the total radio power for our sample. The statistics for this correlation were

TABLE 2

MEANS, MEDIANS, AND MODES IN TOTAL AND RADIO CORE POWERS

Quantity	FR I[a]	FR II[a]	FR II + hz[a,b]	FR II/FR I[c]	FR II + hz[b]/FR I[c]
		$P_{\rm total}$			
Mean[d]	25.50 ± 0.12	26.74 ± 0.11	27.08 ± 0.11	17^{+17}_{-10}	38^{+38}_{-15}
Median[d]	25.38	26.75	26.97	23	38
Mode[d]	25.22	26.78	26.76	37	35
		$P_{\rm core}$			
Mean[e]	23.39 ± 0.11	24.12 ± 0.11	24.10 ± 0.12	6^{+8}_{-5}	5^{+8}_{-5}
Median[e]	23.37	24.05	24.00	5	4
Mode[e]	23.33	23.91	23.74	4	3
Mean (KM)[f]	23.34 ± 0.11	23.97 ± 0.11	24.23 ± 0.11	6^{+8}_{-5}	7^{+8}_{-5}
Number of Upper Limits......	4/81	14/115	27/131	...	...

[a] Radio powers in logarithmic scales.
[b] The term hz stands for high-redshift sources with $z > 0.5$.
[c] Ratios *not* in logarithmic scales.
[d] Data have no upper limits.
[e] Data points with upper limits ignored.
[f] Data with upper limits included, but the means are evaluated using the Kaplan-Meier estimator.

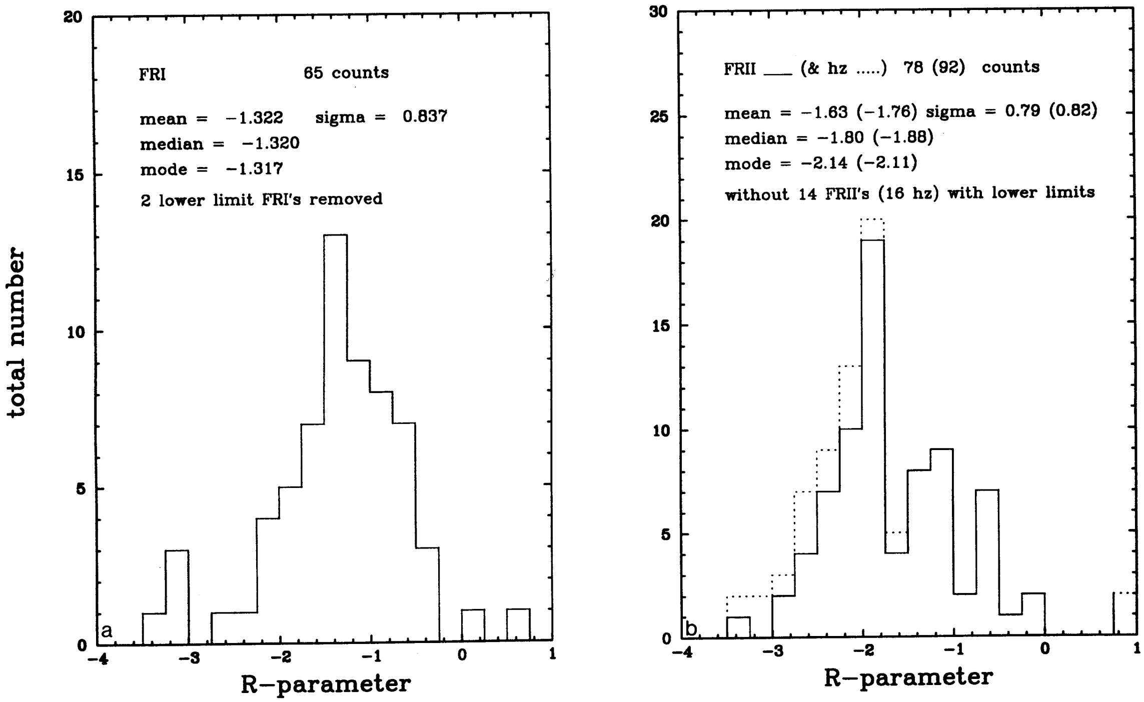

FIG. 5.—Histograms of the R-parameter (the ratio of core to lobe radio fluxes) for (a) FR I's and (b) FR II's. All upper limits were treated as detections in the diagram and means, medians, and modes are quoted. However, if we use the Kaplan-Meier Estimator, we obtain for the FR I's $\langle R \rangle = -1.40 \pm 0.10$; for the FR II's we obtain $\langle R \rangle = -1.91 \pm 0.11$, and for the FR II's including the $z > 0.5$ sources, we obtain $\langle R \rangle = -2.21 \pm 0.11$.

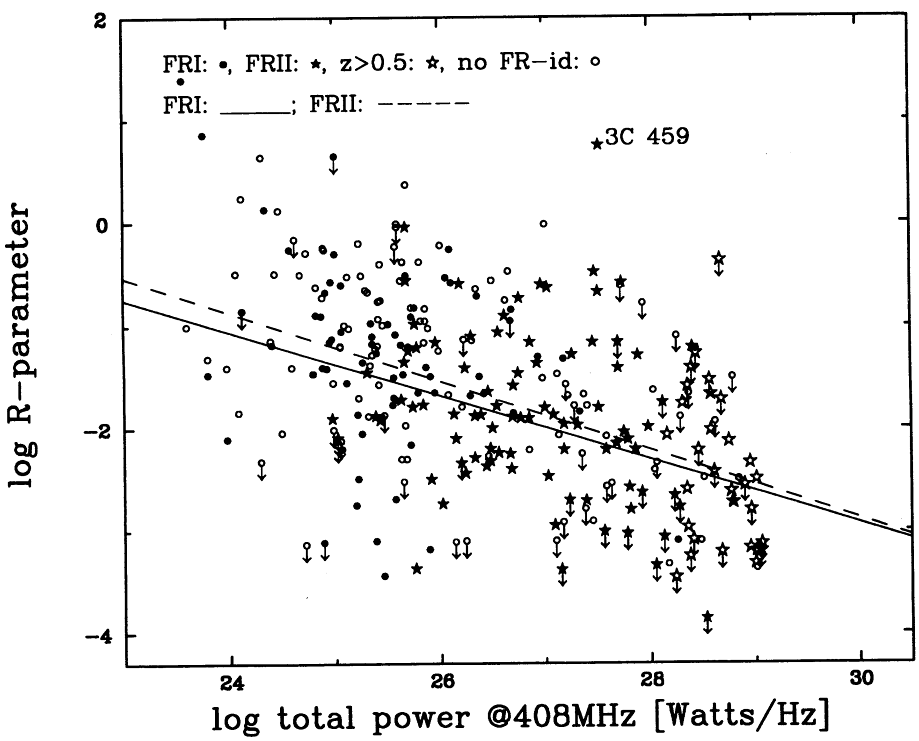

FIG. 6.—Logarithm of total radio power measured at 408 MHz in units of W Hz^{-1} vs. the R-parameter defined by the ratio of core to lobe radio flux. Although we include all radio galaxies that have measured core and total radio powers, we mark those that have been positively identified as FR I's or FR II's as filled circles or filled stars. For the FR I's and the FR II's separately we also show the best-fit lines. Statistics of the fits are listed in Table 3.

TABLE 3

STATISTICS OF THE CORRELATION OF THE *R*-PARAMETER WITH RADIO POWER

Quantity	FR I	FR II	FR II + $z > 0.5$[a]	All Sources
EM Algorithm				
Slope	-0.33 ± 0.12	-0.31 ± 0.11	-0.44 ± 0.08	-0.38 ± 0.05
Intersect	7.14 ± 3.15	6.44 ± 3.00	9.8947	8.45 ± 1.23
Standard Deviation	0.83	0.88	0.86	0.88
Cox Correlation Hazard Model				
χ^2	1.603	11.438	31.30	46.53
Degrees of Freedom	1	1	1	1
Probability	79.5%	99.93%	>99.99%	>99.99%
Kendall's Tau Test				
z-value	1.588	2.613	5.341	7.257
Probability	88.8%	99.1%	>99.99%	>99.99%

NOTES.—Statistics derived using ASURV.
[a] Many of the high-redshift sources have upper limits.

again evaluated using ASURV and are listed in Table 3. We find that the *R*-parameter decreases as a function of total power, consistent with the results by Fabbiano et al. (1984), Fanti et al. (1987), and de Ruiter et al. (1990). However, if we examine the correlation separately for FR I and FR II sources, we find that FR I and FR II sources exhibit the same functional dependence of *R* on the total radio power. To investigate this further, we examine the scatter about the mean relation of *R*-parameter to radio power (using the values in col. [6] of Table 3). In Figure 7 we then display the histograms of the scatter or "adjusted" *R*-parameters of both FR types, and we see immediately that the difference between them is not significant ($\Delta\langle\log R\rangle = 0.005 \pm 0.139$, or 0.010 ± 0.142 if we include measurements with upper limits). Thus, we find: (1) At a fixed total radio power, the FR I's and the FR II's have the same ratio of core to extended radio power; (2) There is a considerable scatter (almost 2 orders of magnitude) about the mean correlation between *R* and total radio power. This scatter is comparable for both FR types.

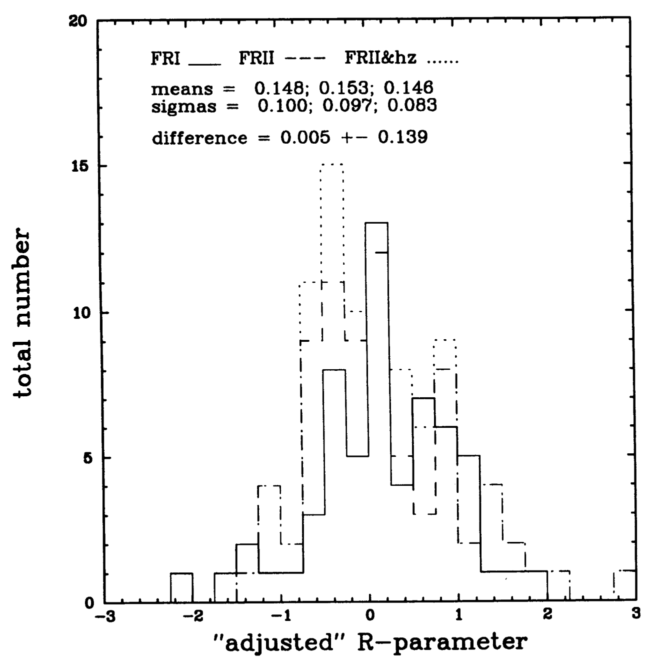

FIG. 7.—"Adjusted *R*-parameter" of (*a*) the FR I's (*solid line*), (*b*) the FR II's (*dashed line*), and (*c*) the FR II's including the $z > 0.5$ sources (*dotted line*). In this plot, we left out all sources with upper limits and find that the difference between the FR I's and the FR II's is 0.005 ± 0.139. When using the Kaplan-Meier Estimator, the difference between the FR I's and the FR II's is 0.010 ± 0.143, i.e., insignificant.

3.2.3. *Evaluation of Systematic Effects*

3.2.3.1. Systematic Errors in Radio Core Powers

In our analysis, the radio core fluxes that we compiled from different references were obtained with different instruments (with the Very Large Array [VLA] using the *A*, *B*, *C*, and *D* arrays, with the Australian Telescope Compact Array [ATCA], with the Westerbrook Synthesis Radio Telescope [WSRT], and with the Cambridge 5K arrays [CA]) and different angular resolutions (typically 1″, 3″, or 13″). Details on which telescopes and which resolutions are used by each group of researchers can be found in the notes section of Table 10. Thus, it is necessary to test whether the radio core fluxes of all groups are compatible. Since the measurements of total radio fluxes are relatively unaffected by those problems (as long as they are measured at the same frequency), the mean *R*-parameter of each group is thus expected to reflect any systematic differences in the radio core power measurements. However, since the *R*-parameter is a function of the total radio power, we need to eliminate this dependence as described in § 3.2.2. We then compare the means of the "adjusted" *R*-parameter of each group of researchers to the mean of the "adjusted" *R*-parameter of all remaining groups. The results are summarized in Table 4. We see immediately that the differences in the means of the adjusted *R*-parameter are statistically insignificant, and thus we conclude that the radio core fluxes of the different groups are compatible.

3.2.3.2. Redshift Selection Effects on *R*

The radio galaxies in the combined sample span a wide range in redshifts ranging from 0.01 to 1.5. To test for any remaining redshift dependence, we correlate the "adjusted" *R*-parameter to redshift and find no correlation even if we include McCarthy's and Morganti et al.'s high-redshift sources. This result has the following implications: (1) The radio core fluxes appear to be insensitive to small variations in angular resolution; (2) There is no detectable evolution in the ratio of

TABLE 4

COMPARISON OF ADJUSTED *R*-PARAMETERS OF VARIOUS GROUPS FOR RADIO SOURCES

Source	Δ Mean[a,b]	σ[a]
Morganti et al. 1992	+0.143	0.207
Morganti et al. 1993; Tadhunter et al. 1993[c]	+0.102	0.143
Giovannini et al. 1988[d]	−0.021	0.089
Caganoff 1988	−0.048	0.146
Baum & Heckman 1989a, b	−0.087	0.141
McCarthy 1988[d]	−0.138	0.114
Rawlings et al. 1989	+0.048	0.108
Total Δ means; mean of total σ's	−0.001	0.135

NOTES.—The different telescopes used by each group of researchers, including the resolution they use to detect the radio core fluxes, can be found in the notes section of Table 1.

[a] Kaplan-Meier estimates which incorporate upper and lower limits.

[b] Δ mean is the difference between in the mean *R*-parameter of this particular group and the mean *R*-parameter of all remaining groups.

[c] The only sources whose *R*-parameters were evaluated from core and total powers measured at 5 GHz. Note that Δ mean is within the 1 σ error of Δ mean.

[d] We excluded all sources with $z > 0.5$.

the core to lobe radio powers; (3) The *R*-parameters are not affected by redshift selection effects.

3.2.4. *The Effects of Beaming on the Radio Core Fluxes*

Lastly, we consider the importance of beaming and orientation effects on these results. In contrast to the total low-frequency radio power, the radio core power may include or be dominated by emission from relativistic jets (e.g., Browne 1983). If this is indeed the case, then the ratio of core to total (or lobe) power could be used as an orientation measurement (e.g., Orr & Browne 1992; Urry, Padovani, & Stickel 1991; Padovani & Urry 1992). To calculate the "expected" contribution due to beaming, we use minimum beaming angles of 20° for FR I's, 40° for FR II's, maximum beaming angles of 90° for both FR types, and mean Lorentz factors of 7 for FR I's and 11 for FR II's (the values are taken from Urry & Padovani 1991). The "expected" scatter due to beaming works out to be in the order of a few hundreds for both the FR I's and the FR II's. However, since we should encounter sources at small beaming angles relatively rarely, the median value of the observed scatter is expected to be considerably smaller. Note that we have excluded BL Lacs and quasars, the unified models of which have the highest values of *R*, from our sample. Our observed scatter, on the order of 100, therefore cannot rule out or constrain beaming arguments. In addition, since the scatter in the *R*-parameters is comparable for both FR types, we conclude that if our sample is contaminated by orientation effects, it happens to the same degree in FR I's as in FR II's.

This result has an important implication for the radio core power versus emission-line luminosity correlation which will be discussed in the next section. There we shall show that the correlations for the FR I's and the FR II's of the emission-line luminosity with core radio power (an orientation-*dependent* measurement) are equally strong as those of the emission-line luminosity with total power (an orientation-*independent* measurement). This suggests that orientation effects are in fact unimportant in our sample.

3.3. *Correlations with Emission-Line Luminosity*

In this section, we examine the relationship of the emission-line luminosity to total radio and core radio power, and we find very different functional dependencies between line and radio luminosity for both FR classes.

3.3.1. *The Emission-Line Correlation with Total Radio Power*

In Figure 8, we display the radio power emission-line correlation for all the radio galaxies in our sample. We have marked the measurements from each group with a different symbol (this means that some sources may appear more than once in this plot). The purpose of showing this plot is twofold: to display the general location of the data from the different groups used in the analysis, and secondly, to show the overall trends. Later in the analysis, we replace multiple measurements by one single measurement as outlined in § 2.5. We note the following: (1) There is a strong correlation between the total radio power and the emission-line luminosity, which is in agreement with previous researchers (Baum & Heckman 1989a, b; Caganoff 1988; McCarthy 1988; Morganti et al. 1992; Rawlings et al. 1989). Both correlation tests, the generalized Kendall's Tau and the Cox Proportional Hazard models, show that the correlation is significant at the 99.9999% level. (2) The correlation extends over a remarkably large range, covering 10 orders of magnitude in radio power and 8 orders of magnitude in emission-line luminosity. (3) There is an indication of a flattening of the slope at the low-power end, but not at the high-power end (see also Baum & Heckman 1989b).

In Figure 9, we again plot emission-line luminosity versus total radio power, but now we have included only one point for each galaxy (see § 2.7), and we have differentiated between FR I's and FR II's. We see the following: (1) Each FR type has its own correlation between emission-line luminosity and the radio power which is significant at least at the 99.99% confidence level (see Table 5). (2) The slopes of the correlations for the FR I's and the low-redshift ($z < 0.5$) FR II's are different (0.28 ± 0.07 and 0.75 ± 0.09, respectively), and none is equal to unity. Note that if we convert the total radio power to jet kinetic energy as done by Rawlings & Saunders (1992), the slope of the FR II's increases to 1.13 ± 0.13, i.e., to almost unity. (4) If we include the high-redshift sources in the sample of the FR II's, the slope steepens at the high-power end rather than leveling off. (5) The mean line of the FR I's goes through the points of the lower power radio galaxies of Sadler et al. (1989). (6) There is an "offset" between the FR II's and the FR I's which is not constant due to the differences in the slopes. This offset can be regarded either as an offset in the total radio power or in the emission-line luminosity, or in both. Thus, FR II's produce 5–30 times more emission-line luminosity than do FR I's of the same radio power. Or, conversely, FR I's produce 10–100 times more total radio power than do the FR II's of the same total line luminosity.

As always, there are a few oddballs that do not fit the general trends. These are labeled in Figure 9. Among the FR I sources with relatively high emission-line luminosities, there are PKS 2322−123, 3C 317, 3C 84, B2 1346+26, B2 0915+33, and B2 1145+35. Note that many of these sources have a very amorphous radio structure (e.g., Baum & Heckman 1989a), and they may thus not be true FR I's. Also, at least some of these sources are known to be in rich clusters, and some are associated with cooling flows (e.g., Heckman et al. 1989) and they may therefore have higher emission-line luminosities. Among the FR II sources with relatively low emission-line activity are 3C 327, 3C 295, 3C 444, and PKS 1654−137. Of these sources, 3C 327 and 3C 295 were already discussed as being different by Baum & Heckman (1989a), and PKS 1654−137 may be misclassified,

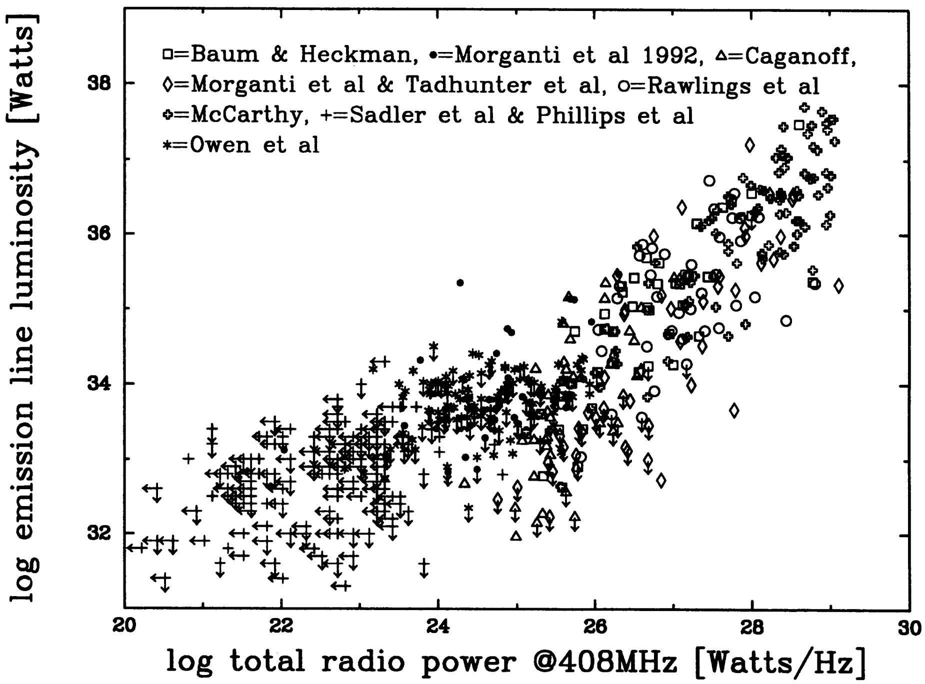

FIG. 8.—Logarithm of total radio power measured at 408 MHz in units of W Hz^{-1} vs. the logarithm of the Hα + [N II] emission-line luminosity measured in watts. We display all data that we compiled and mark the data of each group of researchers with different symbols. Note that some galaxies may appear more than once in this plot.

as it belongs to Caganoff's sample, or it may have a spurious emission-line luminosity because the emission lines are powered by the ISM. Note that although 3C 295 is in a rich cluster, it does not have an anomalously high emission-line luminosity. Therefore, the connection between an enhanced emission-line luminosity and cluster membership or X-ray luminosity is uncertain and needs further study.

3.3.2. *The Emission-Line Luminosity Correlation with Radio CORE Power*

In Figure 10, we plot radio core power versus emission-line luminosity for all galaxies in our sample. In this plot, we have marked the measurements from the various researchers by different symbols, and we note that some galaxies may have been included in this plot more than once. Again, the intention is to

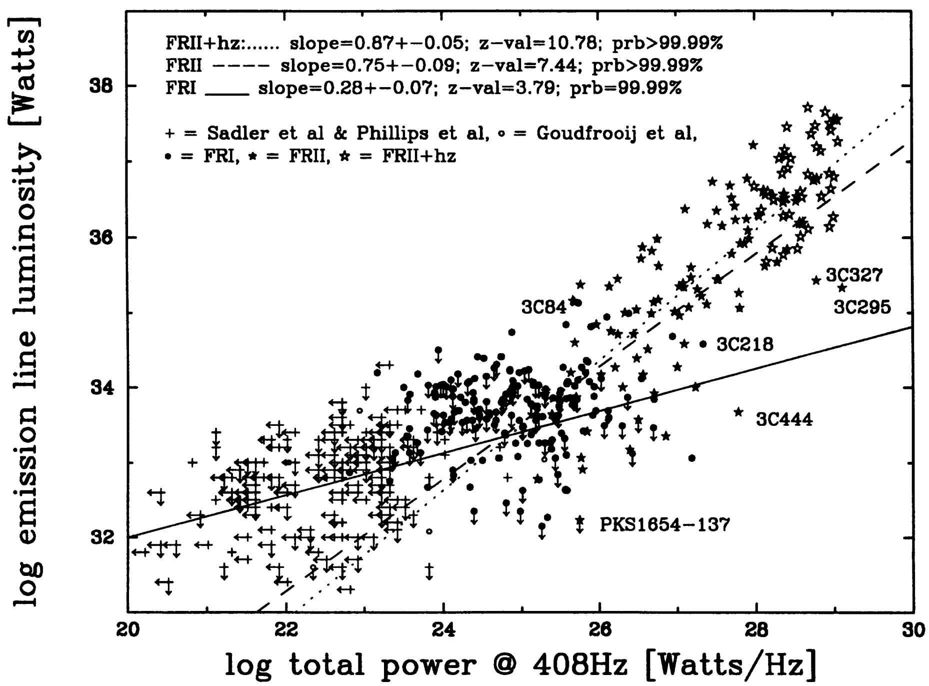

FIG. 9.—Logarithm of total radio power measured at 408 MHz in units of W Hz^{-1} vs. the logarithm of the Hα + [N II] emission-line luminosity measured in watts. We distinguish between FR I, FR II, and high-redshift FR II sources and the weaker sources from Sadler et al. (1989). We also mark FR I's and FR II's which do not follow the "normal" trend. Statistics for the fits are listed in Table 5.

TABLE 5

STATISTICS OF THE CORRELATION OF LINE LUMINOSITY WITH RADIO POWER

Quantity	FR I	FR I + Sadler	FR II[a]	FR II + $z > 0.5$[a]
		EM Algorithm		
Slope	0.28 ± 0.07	...	0.75 ± 0.08	0.86 ± 0.05
Intersect	26.34 ± 1.83	...	14.78 ± 2.34	11.86 ± 1.50
Standard Deviation	0.71	...	0.79	0.71
		Cox Correlation Hazard Model		
χ^2	9.649	...	44.44	105.58
Degrees of Freedom	1	...	1	1
Probability	99.81%	...	>99.99%	>99.99%
		Kendall's Tau Test		
z-value	3.794	8.925	7.338	10.781
Probability	99.99%	>99.99%	>99.99%	>99.99%
		Schmitt's Method		
Slope	0.34 ± 0.13	0.24 ± 0.05	...	...
Intersect	24.62 ± 3.11	26.85 ± 1.04	...	...

NOTE.—Statistics derived using ASURV.

[a] We distinguish between the lower ($z < 0.5$) and the higher ($0.5 < z < 1.5$) radio sources. We do this in order to isolate evolutionary effects (see § 2.4), and because the emission-line luminosities of the higher power sources were calculated by transforming [O II] and [O III] to Hα + [N II].

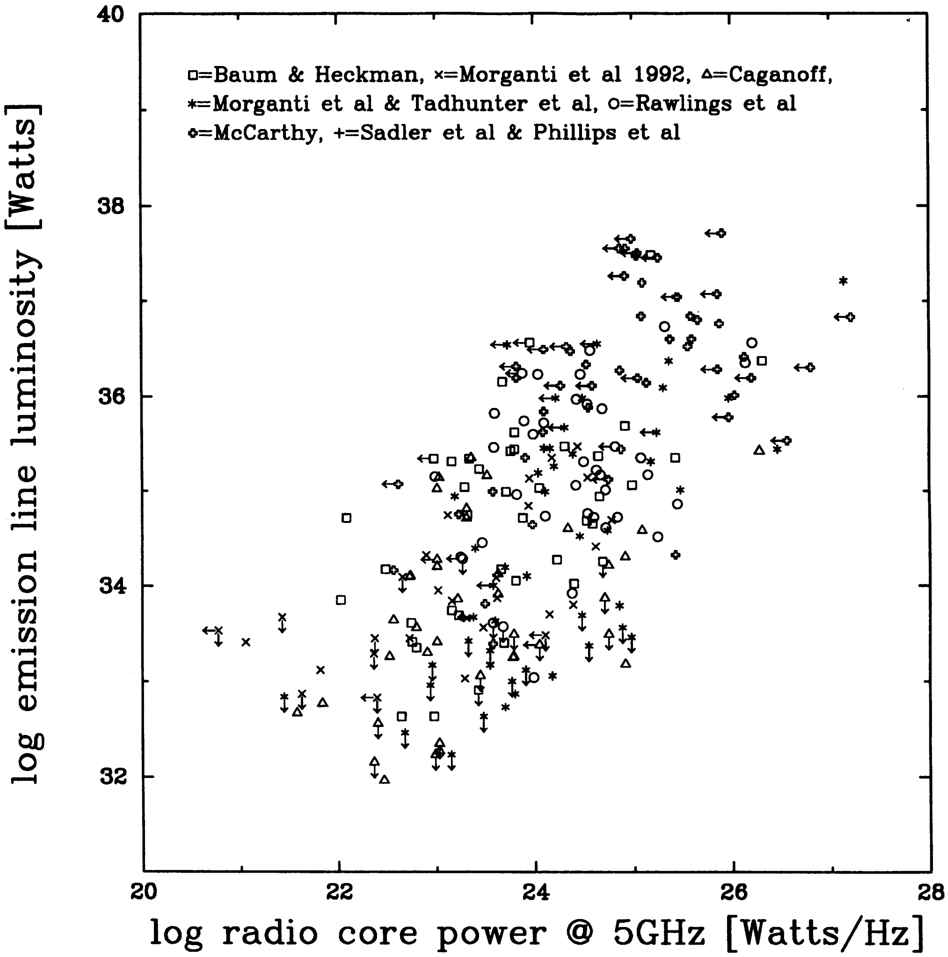

FIG. 10.—Logarithm of radio core power measured at 5 GHz in units of W Hz^{-1} vs. the logarithm of the Hα + [N II] emission-line luminosity measured in watts. We display all data that we compiled and mark the data of various groups of researchers with different symbols. Note that some galaxies may appear more than once in this plot.

show the overall scatter and the regions occupied by the different groups of researchers whose data we use. We find that the overall correlation of core power with line luminosity is weaker than the corresponding correlation between total power and line luminosity, as already noted by Baum & Heckman (1989b) and by Rawlings et al. (1989). However, this changes if we differentiate between the two FR types.

In Figure 11, we plot the radio core power versus emission-line luminosity for both FR types (here each galaxy has only one measurement). Note that Sadler et al.'s and Goudfrooij et al.'s radio galaxies are marked by a different symbol in Figure 11 and are not included in the statistics (Table 6). We find the following: (1) Each FR type has its own independent correlation of core power with line luminosity. (2) The correlations of emission-line luminosity with radio core power are equally strong as those with total radio power if we distinguish between the FR I's and the FR II's. (3) The slopes of the FR I's and the FR II's are different (0.3710.12 and 0.6210.10, respectively). (4) The FR I's and the FR II's separate out more clearly in the emission-line luminosity versus core power plot than in the emission-line luminosity versus total power plot. This offset is not constant due to the differences in the slopes, and it can be regarded either as an offset in the total radio power or in the emission-line luminosity, or in both. Thus, for the same radio core power as the FR I's, the FR II's produce consistently about 10–50 times as much emission-line luminosity; or, for the same amount of emission-line activity as the FR II's, the FR I's produce about 200–300 times as much radio core power.

3.4. *Correlations with Host Galaxy Optical Magnitude*

In this section we examine the three-way correlations of line luminosity with the host galaxy optical magnitude and with radio luminosity. We find that the FR I's and radio-quiet galaxies have a comparable line luminosity–magnitude relationship, but that the FR I's have on average slightly higher emission-line luminosities. If we remove the correlation of line luminosity on optical magnitude, we find a residual correlation between line luminosity and radio luminosity for the FR I sources which is only significant at the 2 σ level.

3.4.1. *Correlation of Emission-Line Luminosity with Host Galaxy Optical Magnitude*

In Figure 12*a*, we plot absolute optical magnitude of the host galaxy versus line luminosity for the FR I's, including the comparison sample of optically selected galaxies. In Figure 12*b*, we plot the same parameters, this time for the FR II's, where we have separately indicated the high-redshift and low-

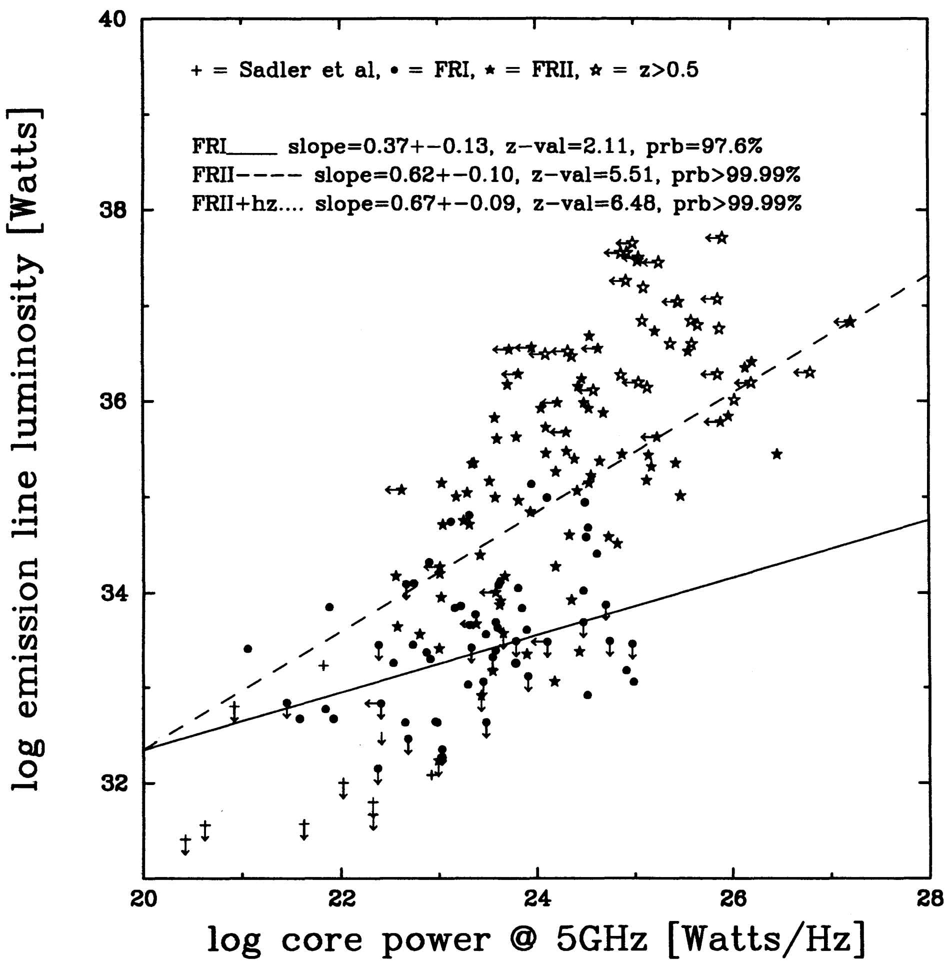

FIG. 11.—Logarithm of radio core power measured at 5 GHz in units of W Hz^{-1} vs. the logarithm of the Hα + [N II] emission-line luminosity measured in watts. We distinguish between FR I, FR II, and FR II + hz sources. Also, we display some of Sadler et al.'s and Goudfrooij et al.'s sources if radio core powers exist but mark them with a different symbol. Note that we only present one single measurement for each radio source. Statistics are listed in Table 6.

TABLE 6

STATISTICS OF THE CORRELATION OF LINE LUMINOSITY WITH RADIO CORE POWER

Quantity (1)	FR I (2)	FR I[a] (3)	FR II (4)	FR II[b] (5)	FR II + $z > 0.5$ (6)
Number of Points	61	59	81	82	112
Upper Limits in x	16	16	2	3	2
Upper Limits in y	2	0	12	12	28
Limits in Both	2	0	0	0	0
		EM Algorithm			
Slope	...	0.30 ± 0.12	0.66 ± 0.10	0.62 ± 0.10	0.66 ± 0.09
Intersect..................	...	26.3 ± 2.8	18.9 ± 2.4	19.9 ± 2.3	18.9 ± 2.1
Standard Deviation......	...	0.79	0.84	0.80	0.86
		Schmitt's Method			
Slope[c]	0.29 ± 0.12	0.37 ± 0.13	0.61 ± 0.12	0.62 ± 0.12	0.60 ± 0.11
Intersect[c]..................	26.1 ± 2.8	24.9 ± 2.9	20.3 ± 2.9	19.8 ± 2.8	20.3 ± 2.6
		Cox Correlation Hazard Model			
χ^2	...	3.67	34.91	31.27	41.70
Probability	...	96%	>99.99%	>99.99%	>99.99%
		Kendall's Tau Test			
z-value	2.338	2.113	5.698	5.515	6.48
Probability	88.1%	97.6%	>99.99%	>99.99%	>99.99%

NOTES.—Statistics derived using ASURV. We trust the data in cols. (3), (5), and (6) more than those in cols. (2) or (4).

[a] Two data points of 58 FR I's with upper limits in both quantities are ignored.

[b] One data point which is most likely spurious (PKS 1654) of 81 FR II's is ignored.

[c] Bootstrap approximation using 200 iterations, x bins = 10, y bins = 5, and seed = −1.

redshift FR II's and where we have again included the optically selected galaxies from our comparison sample. We then compute correlation statistics for various subsets of the data displayed in these figures. The statistics of all correlations are listed in Table 7. We find: (1) For the FR I's the optical magnitude correlates with line luminosity (at the 99.93% level) in the sense that the optically more luminous galaxies have higher emission-line luminosities. (2) the low-redshift FR II's show no correlation between absolute magnitude and the emission-line luminosity. However, we do find a correlation for the FR II's if we include the high-redshift FR II's (significant at the 99.99% level). The nature of this correlation may have its origin in a strong contribution to the optical magnitude from a nuclear nonthermal component, from scattered nuclear light, or from inverse Compton scattering from the radio source (Daly 1992). (3) At a fixed absolute V magnitude of −23.3 (which corre-

TABLE 7

STATISTICS OF THE CORRELATION OF LINE LUMINOSITY WITH MAGNITUDE SEPARATELY FOR THE FR I'S AND THE FR II'S

Quantity	FR I's	Low-z FR II's[a]	All FR II's[b]
Number of Points	156	53	81
Limits in y................	76	0	0
	EM Algorithm		
Slope	-0.26 ± 0.09	0.10 ± 0.18	-0.46 ± 0.08
Intersect..................	27.3 ± 2.0	37.4 ± 4.2	24.1.8
Standard Deviation......	0.73	0.94	0.92
	Cox Correlation Hazard Model		
χ^2	5.988	0.039	34.086
Probability	98.56%	35.49%	>99.99%
	Kendall's Tau Test		
z-value	3.385	0.368	5.001
Probability	99.93%	28.74%	>99.99%

NOTE.—Statistics derived using ASURV.

[a] All FR II's with redshifts below 0.5 were used.

[b] All FR II's with redshifts below 1.5 were used, i.e., high-redshift FR II's are included.

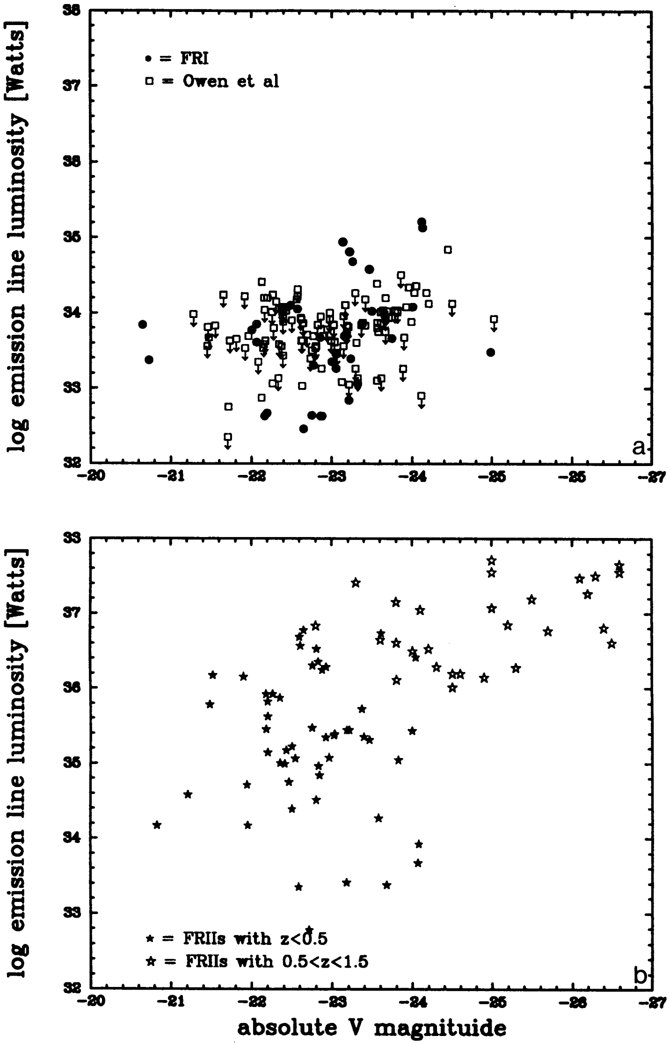

FIG. 12.—Absolute V magnitude vs. logarithm of emission-line luminosity for (*a*) FR I's (*filled circles*) and Owen et al.'s FR I's (*squares*) and (*b*) FR II's (*filled stars*). Note that the low-redshift ($z < 0.5$) FR II's show no correlation. Statistics are listed in Table 7.

sponds to the mean magnitude of brightest cluster members, e.g., Sandage 1972a, b), FR II's emit about 100 times as much emission-line luminosity as FR I's.

It is most important to compare the correlation of line luminosity with absolute magnitude of the FR I radio galaxies to that of "radio-quiet" galaxies. In Figure 13 we display the emission-line luminosity absolute magnitude correlation for FR I sources as well as that for radio-quiet galaxies, and in Table 8 we list the statistics. We find that: (1) The slopes of the correlations for radio-quiet ellipticals and FR I galaxies are almost comparable (-0.36 ± 0.05 and -0.26 ± 0.09, respectively). (2) The FR I sources occupy the region of higher emission-line luminosities. The difference in the mean emission-line luminosity between FR I's and radio-quiet galaxies is $\Delta \log L_{\rm line} = 0.8 \pm 0.1$; however, the scatter in the mean line luminosity is as large as the difference.

3.4.2. *The Three-Way Correlation between Line Luminosity, Radio Power, and Magnitude*

To test whether there is a "residual" correlation of line luminosity with radio power, we need to remove the magnitude dependence from the emission-line luminosity. We adjust the emission-line luminosities of the FR I's by using the values from the third column of Table 8, and we evaluate the corresponding emission-line luminosity by requiring that they have an absolute magnitude of $M_V = -23.3$ (this magnitude corresponds to the absolute magnitude of brightest cluster members, e.g. Sandage 1972a, b). Similarly, we remove the magnitude dependence from the Sadler et al. radio galaxies by using the fourth column of Table 8. We then correlate the "adjusted" emission-line luminosity against the radio powers for both the FR I's and the Sadler et al. sources. This is displayed in Figure 14, and the statistics are listed in Table 9. For the FR I's, the slope is reduced from 0.34 ± 0.13 (for the "raw" correlation between line and radio luminosity) to 0.25 ± 0.14 (for the "adjusted" correlation). However, the resulting "adjusted" correlation is only significant at the 2 σ level. If we include the Sadler et al. sources among the FR I's, the slope is reduced from 0.24 ± 0.5 to 0.13 ± 0.04, but the adjusted correlation is still only significant at the 3 σ level.

If we perform a similar test for the FR II sources and we adjust the emission-line luminosities by using the values of column (6) of Table 7, we find that the residual correlation still has a statistically significant slope. Thus, the correlation for the FR II's between radio and line luminosity is real.

4. SUMMARY

We know from previous work that there are substantial differences between powerful FR I's and FR II's. Not only are the host galaxies (Smith 1988; Baum et al. 1992; Heckman et al. 1994; Zirbel 1994a) and the megaparsec-scale environments (Prestage & Peacock 1989; Hill & Lilly 1991; Zirbel 1994b) different, but there are also fundamental differences in the smaller scale environments of the emission-line regions (e.g., Longair & Riley 1979; Caganoff 1988; McCarthy 1988; Baum & Heckman 1989a, b; Rawlings et al. 1989; Saunders et al. 1989; Morganti et al. 1992; Rawlings & Saunders 1992). In this paper we tried to analyze various interrelationships between the total radio power, the radio core power, the Hα and [N II] emission-line luminosity, and the absolute magnitude. In Paper II we shall discuss the implications of these results for our understanding of the origin of the FR I/FR II dichotomy. To summarize, we list our principal results.

Correlating core power to total power, we find the following:

1. The difference between the radio core powers of FR I's and FR II's is less than the difference between the extended radio powers: the median total radio powers of the FR II's in our sample are about 40 times greater than those of the FR I's, while the median radio core powers of the FR II's in our sample are only about 4 times greater than those of the FR I's.
2. In agreement with previous work, we find a decrease (with slope -0.38 ± 0.05) in the ratio of core to lobe radio power, the R-parameter, with increasing total radio power. The correlation probability is better than 99.99%.
3. The scatter in the R-parameter is significant (about 2 orders of magnitude).
4. At fixed total radio power, the FR I's and the FR II's have the same ratio of core to lobe power and also the same scatter.

Investigating systematic effects on the above results, we find:

1. Redshift selection effects do not affect the R-parameter, and there is no detectable evolution in the R-parameter up to redshifts of 1.5.

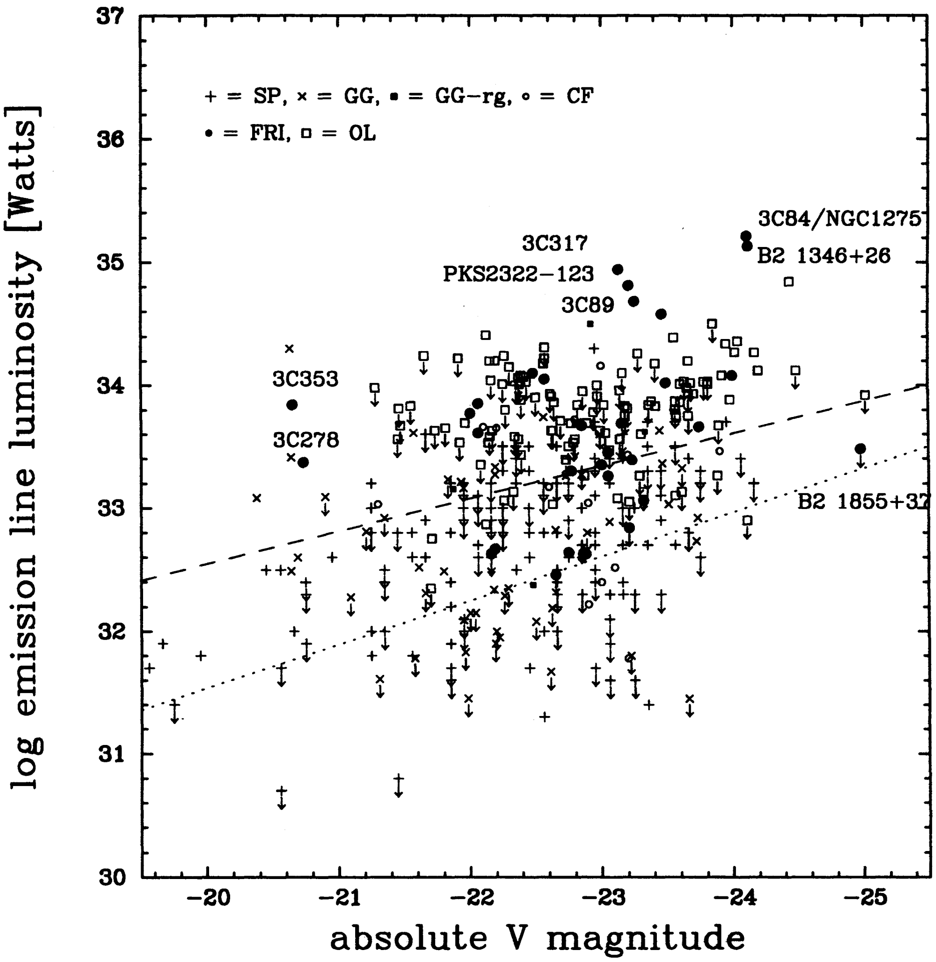

FIG. 13.—Comparing the correlation of absolute magnitude with the logarithm of the emission-line luminosity of radio-loud to radio-quiet galaxies. Phillips et al.'s galaxies are denoted by " +," Goudfrooij et al.'s galaxies are denoted by " ×," and cooling flow galaxies are denoted by " ○," Owen et al.'s FR I's are open squares, and the others are filled circles. FR I sources of special interest are labeled. Statistics for the fits are listed in Table 8.

TABLE 8

STATISTICS (USING ASURV) OF THE CORRELATION OF LINE LUMINOSITY WITH MAGNITUDE

Quantity (1)	FR I's ONLY Radio-loud (2)	G&G + S&P[a] Radio-quiet (3)	FR I + S + GG + CF[b,c] Radio-loud and Radio-quiet (4)
Number of Points	156	215	371
Limits in y	76	95	171
	EM Algorithm		
Slope	−0.26 ± 0.09	−0.39 ± 0.53	−0.45 ± 0.05
Intersect..................	27.3 ± 2.0	23.6 ± 1.2	22.5 ± 1.1
Standard Deviation......	0.73	0.83	0.90
	Cox Correlation Hazard Model		
χ^2	5.988	19.157	37.089
Probability	98.56%	>99.99%	>99.99%
	Kendall's Tau Test		
z-value	3.385	5.093	7.119
Probability	99.93%	>99.99%	>99.99%

NOTE.—Statistics derived using ASURV.
[a] Goudfrooij et al.'s 1993, 1994 galaxies and Sadler et al.'s 1986 galaxies.
[b] FR I galaxies, Sadler et al.'s galaxies, Goudfrooij et al.'s galaxies, and cooling flow galaxies.
[c] Means are taken for overlapping sources as described in § 2.6.

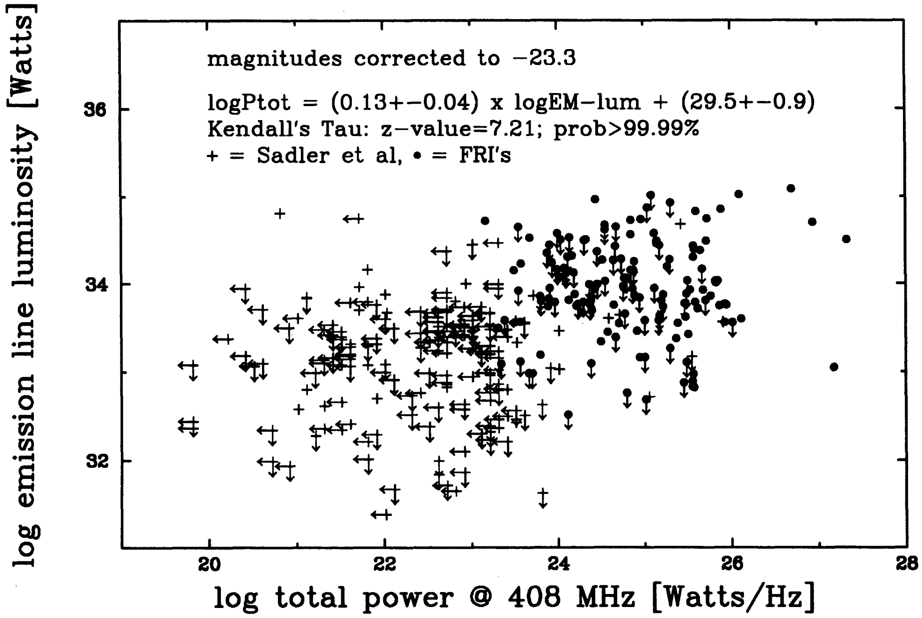

FIG. 14.—Logarithm of total radio power measured at 408 MHz in units of W Hz^{-1} vs. the logarithm of the "adjusted" Hα + [N II] emission-line luminosity measured in watts for FR I sources and the Sadler et al. sources (see text for explanations of how and why this adjustment was applied). Statistics are listed in Table 9.

2. The effects of orientation and beaming on the R-parameter are either much smaller than the intrinsic scatter in the R-parameter or they themselves may produce that scatter. Since the scatter is the same for FR I and FR II sources, beaming effects must be equally important or equally unimportant in both FR types.

We analyze the three-way correlation between redshift, radio power, and emission-line luminosity and find that the correlation of radio power with redshift is stronger than that of emission-line luminosity with redshift. Thus, although our sample is contaminated by the "artificial" radio power redshift correlation, the correlation of radio power with emission-line luminosity is at least partially real. Differentiating between FR I's and FR II's, we find:

1. The FR I's show virtually no correlation between line luminosity and redshift.

2. For the FR II's, the correlation between line luminosity and redshift is stronger than that for the FR I's, which may be either due to an evolutionary effect, or more likely is due to a steeper radio power emission-line luminosity correlation.

When correlating the total radio power to the emission-line luminosity, we show that this correlation extends an even larger range than previously thought, over 8 orders in magnitude in emission-line luminosity and over 10 orders of magnitude in total radio power. Differentiating between FR I's and FR II's, we find:

1. Each FR type has its own correlation between the radio power and the emission-line luminosity; the correlation probabilities are both better than 99.99%.

2. The slopes for the FR I's and the FR II's are different, and neither is unity. (a) The slope for the correlation of the FR II's is 0.75 ± 0.09. If there are no strong evolutionary effects and if

TABLE 9

RADIO POWER STATISTICS

PARAMETER	FR I Raw	FR I Adjusted	FR I + SADLER et al. Raw	FR I + SADLER et al. Adjusted
	Schmitt's Test			
Slope	0.34 ± 0.13	0.25 ± 0.14	0.24 ± 0.05	0.13 ± 0.04
Intersect	24.6 ± 3.1	26.8 ± 3.4	26.8 ± 1.0	29.5 ± 0.9
	Kendall's Tau Test			
z-value	3.794	2.817	8.925	7.214
Probability......	99.99%	99.51%	>99.99%	>99.99%

NOTE.—Statistics of the radio power vs. the "raw" emission-line correlation and the "adjusted" emission-line correlation for FR I sources and for FR I's and Sadler et al.'s sources.

The correlation of the FR I's was adjusted using col. (2) of Table 8, while the correlation for the FR I's + Sadler et al.'s sources was adjusted using col. (4) of Table 8.

we can include higher redshift sources (with $z > 0.5$), the slope rises to 0.87 ± 0.05 (b) The slope for the FR I's is shallower (0.28 ± 0.7).

3. There is an "offset" between the FR II's and the FR I's which is not constant due to the difference in slopes. Nevertheless, it can be described in two fashions: for the same total radio power as the FR I's, and FR II's produce consistently about 5–30 times as much emission-line luminosity; or for the same amount of emission-line activity as the FR II's, the FR I's produce about 10–100 times as much total radio power.

Correlating the core radio powers to the emission-line luminosities, we find:

1. Each FR type has its own correlation between the radio core power and the emission-line luminosity. The correlation probabilities of each FR type are as good as in the correlation probabilities of the total radio power with the emission-line luminosity.

2. The slopes for both correlations are again different. The slope is 0.62 ± 0.10 for the FR II's (0.67 ± 0.09 including the $z > 0.5$ sources) and 0.37 ± 0.12 for the FR I's.

3. The two FR types separate out more clearly than in the total power versus emission-line plot. We describe the variable "offset" in two fashions: for the same radio core power as the FR I's, the FR II's produce consistently about 10–50 times as much emission-line luminosity; or, for the same amount of emission-line activity as the FR II's, the FR I's produce about 200–300 times as much radio core power.

When correlating the emission-line luminosity to the absolute magnitudes of FR I's, FR II's, and optically selected galaxies, we find:

1. The line luminosity correlates with optical magnitude for FR I's alone and for the combined sample of FR I's and optically selected galaxies. Removing the correlation of line luminosity on optical magnitude, we find a residual correlation of line luminosity on radio luminosity whose slope is almost flat (0.25 ± 0.14) and significant at the 2 σ level.

2. The line luminosity does not correlate with optical magnitude for low-redshift FR II galaxies, and the FR II radio galaxies emit appreciably greater quantities of line luminosity than do optically selected galaxies of the same optical magnitude (e.g., at $V = -23.3$, FR II's emit, in the mean, 100 times as much line luminosity as do optically selected ellipitical galaxies).

3. Line luminosity does correlate with optical magnitude for FR II radio galaxies if we look exclusively at FR II galaxies *and* include the high-redshift ($z > 0.5$) and high–radio luminosity ($P_{408\,\mathrm{MHz}} > 10^{27}$ W Hz^{-1}) sources. This may reflect a strong nonthermal (nuclear) contribution to the optical magnitude for these high-redshift, high-power sources.

The bottom line of this analysis is that the "classical" FR I's and the "classical" FR II's are very different in the ratio of line to radio luminosity which they produce. At the same time, we found that at a fixed total radio power, the FR I's and FR II's are similar in the ratio of core to total power which they produce. In summary, the differences between the FR I's and the FR II's go beyond differences in the megaparsec environments and differences in the properties of the host galaxies. In a companion paper (Paper II), we discuss the implications of these results for our understanding of the FR I/FR II dichotomy. There we address the question of whether these differences are due to a difference in the properties of the immediate surroundings of the nuclear engine, or whether the engines themselve are fundamentally different.

We want to thank Gus Oemler, Tim Heckman, and Chris O'Dea for their input in the early stages of this work. We also wish to thank Alessandro Capetti, Frazer Owen, Meg Urry, Dave De Young, and Paul Wiita for fruitful discussions and suggestions and the referee and Chris O'Dea for careful reading of the document. The ASURV package of the astronomical survival analysis was generously made available by E. Feigelson. We acknowledge the services provided by the NASA Extragalactic Database, NED. Partial support for this work was provided by NASA grant NAF-526555.

APPENDIX

Table 10 gives a summary of data compiled from various sources, and Table 11 presents the final list of radio galaxies. The key to the notes to Table 10 is as follows:

Note (*1*).—Baum & Heckman (1989a, b) list extended radio fluxes with $S_{408\,\mathrm{MHz}} > 11$ Jy on the Baars et al. (1977) flux density system. Their narrow-band filters in Hα + [N II] are typically 80 Å wide, and the adopted fluxes are dereddened emission-line fluxes. Their radio core fluxes are measured at 6 cm using the VLA A, B, C, D arrays with the aim to obtain a resolution of $\sim 1''.2$ for each source. They compile other radio core fluxes from the literature for one-fourth of their sources which were measured at 21 cm and 2 cm.

Note (*2*).—We use Caganoff's (1988) 5 GHz radio core fluxes, and from his 1.4 GHz extended radio fluxes we calculate the 408 MHz extended fluxes using a mean spectral index of 0.75. Even though he states emission-line luminosities in several lines, we only adopt those measured in Hα + [N II]. His fluxes are obtained from slit spectroscopy (see § 2.1). Due to unknown inconsistencies, we reclassified his sources according to the FR scheme from the radio maps that he provided in his thesis.

Note (*3*).—Depending on the redshift of the object, McCarthy (1988) either measured Hα + [N II], [O II], or [O III], and we converted all high-redshift sources (with $z > 0.5$) which are presumably FR II's to Hα + [N II] via [O II]/(Hα + [N II]) = 4.0 and [O III]/(Hα + [N II]) = 1.1.

Note (*4*).—Giovannini et al. (1988) used many of Feretti et al.'s (1984) core powers and obtained 36 new observations with the VLA A array. They obtained their extended radio fluxes from Colla et al. (1975a, b). They took M_{vis} from Meier et al. (1979) or Spinrad et al. (1985), and we estimate that their maximum uncertainties lie in the order of a few tenths of a magnitude.

Note (*5*).—Morganti et al. (1992) compiled their core powers from Giovannini et al. (1988) and Feretti et al. (1984) and obtained remaining ones with the Westerbrook Synthesis Radio Telescope. They list total Hα + [N II] fluxes measured by themselves, where

TABLE 10

SUMMARY OF DATA AND CORRESPONDING REFERENCES[a]

P_{total}	P_{core}	Emission Lines[b]	Reference	Notes
408	5000[c]	Hα + [N II], [O II]	Baum & Heckman 1989a, b	1
1400, 2700[d]	5000	Hα + [N II][e]	Caganoff 1988	2
178	n/a	Hα + [N II], [O II], [O III]	McCarthy 1988	3
408	5000	n/a	Giovannini et al. 1988	4
408	5000	Hα + [N II]	Morganti et al. 1992	5
5000	5000	n/a	Morganti et al. 1993	6
n/a	n/a	[O II], [O III]	Tadhunter et al. 1993	7
408	5000	n/a	Feretti et al. 1984	8
178	5000	[O III]	Rawlings et al. 1989	9
178	n/a	Hα + [N II]	Rawlings & Saunders 1992	10
5000	n/a	n/a	Sadler et al. 1989	11
n/a	n/a	Hα, N [II][e,f]	Phillips et al. 1986	12
1400	n/a	n/a	Rowan-Robinson et al. 1993	13
n/a	n/a	Hα, separately [N II]	Benn et al. 1993	14

[a] The frequencies are given in MHz.

[b] For simplicity we abbreviate [O III] λ4959/5007 by [O III], [O II] λ3727 by [O II], and Hα + [N II] λλ6584, 6548 by Hα + [N II]. In the rest of the analysis, we abbreviate Hα + [N II] λλ6584, 6548 further to Hα.

[c] Baum & Heckman mostly quote the 5 GHz fluxes, but in one-fourth of their data they compile the core fluxes from other references which are measured at 21 or 2 cm (see notes above).

[d] The *R*-parameter is calculated by transforming the extended 2.7 GHz fluxes to 5 GHz, but the extended radio luminosities are calculated from the measurements at 1.4 GHz.

[e] Emission-line fluxes obtained from slit spectra; all other fluxes are obtained via imaging.

[f] Phillips et al. list Hα and Hα + [N II] separately; we use their Hα + [N II] fluxes.

they use narrow-band filters (50 Å) adjusted to the redshifts of the objects; continua were subtracted. They use the extended radio fluxes computed by Colla et al. (1975).

Note (*6*).— Morganti et al. (1993) obtained both their extended and their radio core fluxes with the VLA B and C arrays and the ATCA. They then derive radio morphologies from the extended 5 GHz radio maps. Note that the FR morphologies of all other radio galaxies have been obtained from lower frequency radio maps.

Note (*7*).—Tadhunter et al. (1993) list O [III] for all their sources which are the same sources as in Morganti et al.'s (1993) sample. Whenever the radio morphology is known for those sources (FR identifications are obtained from Morganti et al. 1993), we transformed the O [III] fluxes of the FR II's to Hα + [N II] via [O III]/(Hα + [N II]) = 1.1 and of the FR I's via [O III]/(Hα + [N II]) = 1.2 ± 0.5 (see § 2.1).

Note (*8*).—Feretti et al.'s (1984) core powers are obtained with the VLA A array. Their extended radio fluxes are adopted from Colla et al. (1975). They obtained M_{vis} from Meier et al. (1979) or Spinrad et al. (1985), as did Giovannini et al. (1988).

Note (*9*).—Rawlings et al. (1989) use total radio powers measured at 178 MHz Baars et al. scale. Since they quote spectral indices between 178 and 750 MHz, it is straightforward to convert their $P_{178\,\mathrm{MHz}}$ measurements to $P_{408\,\mathrm{MHz}}$. Their core radio fluxes are all measured at 5 GHz. Their emission-line luminosities are measured in [O III], and for those sources for which we could find FR classifications, we transformed the fluxes of the FR II's to Hα + [N II] via [O III]/(Hα + [N II]) = 1.1 and the FR I's via [O III]/(Hα + [N II]) = 1.2 ± 0.5 (see § 2.1). All their emission-line luminosities are corrected for galactic extinction.

Note (*10*).—From total radio powers, equiparticipation arguments, and radio lobe expansion arguments, Rawlings & Saunders (1992) estimate the kinetic jet energy. Rawlings & Saunders take their Hα + [N II] line luminosities from Rawlings et al. (1989), Jackson & Browne (1989), and McCarthy (1988).

Note.—(*11*).—Sadler et al. (1989) measure the total radio fluxes for sources with $S_{5\,\mathrm{GHz}} > 0.8$ (using the VLA hybrid B/C configurations). They note that each galaxy was observed at least at the 5 σ detection limit, and in a few cases they were able to detect the extended radio emission. They computed optical *B* magnitudes from ESO 137-G0 plates and the PKS/VLA sample; high reddening galaxies were excluded. We estimate that the accuracy of their magnitudes should be within three-tenths of a magnitude. Assuming the galaxies are mostly ellipticals or SO's, we convert their *B* magnitudes to *V* assuming $B-V = 0.95$. The Hα luminosities were obtained from the Phillips et al. sample.

Note (*12*).—Phillips et al. (1986) detect both Hα and [N II] separately and find that in most cases the ratio of Hα/ [N II] varies between 1 and 3. For consistency reasons, we take their Hα + [N II] luminosities and evaluate the Hα + [N II] luminosity from their data, whenever this information is not listed. The emission-line luminosities are combined with the radio properties of the Sadler et al. (1989) paper. All their emission-line fluxes are obtained by slit spectra, but since they are faint radio sources with relatively little emission-line gas which is mostly contained within 2.5 kpc of the nucleus (see Baum & Heckman 1989b), we consider their emission-line fluxes acceptable (see § 2.1).

Note (*13*).—Rowan-Robinson et al.'s (1993) sample is complete to $S_{1.4\,\mathrm{GHz}} \geq 0.1$ mJy. However, in contrast to all other radio galaxies, they include faint radio emitters that extend to relatively high redshifts.

Note (*14*).—Benn et al. (1993) obtained spectroscopy for the Rowan-Robinson et al. (1993) sample. They calculate the *B*/*V* absolute magnitudes from the rest frame 5000 Å flux density; colors are also listed in their reference in terms of the 5000 Å/7000 Å and 7000 Å/9000 Å, but none are used in this paper. Only objects identified as elliptical galaxies were included in our analysis, and unfortunately none of these had measurable emission-line luminosities.

TABLE 11

SAMPLE OF RADIO-LOUD ELLIPTICAL GALAXIES[a]

Name (1)	IAU (2)	redshift (3)	magnitude (4)	α (5)	P_{total} (6)	P_{core} (7)	Line-Lum (8)	FR (9)	$R=P_l/P_c$ (10)	Reference (11)
3C 6.1	0013+79	0.840	-24.50	0.80	28.58	26.03	36.01	H	-1.67	MC,G
PKS 0023-26	0023-26	0.322	...	0.70	28.04	...	...	U	...	MT
3C 13.0	0031+39	1.351	-26.20	0.93	29.06	<24.92	37.26	H	<-3.13	MC,G
3C 15	0034-01	0.073	-22.95	0.60	26.35	24.86	33.79	I/II	-0.64	Z,MT
B2 0034+25	0034+25	0.032	...	...	24.07	22.64	...		-0.49	G
3C 17	0035-02	0.220	-22.40	0.52	27.48	26.11	...	I/II	-0.48	Z,LRL,MT
3C 16	0035+13	0.405	-22.24	0.94	27.56	<23.73	...	II	<-3.01	G,Z
3C 18	0038+09	0.188	-23.46	0.74	27.26	25.18	35.31	II	-1.28	Z,MT
3C 19.0	0038+32	0.482	...	...	27.94	<26.27	...		<-0.78	G
PKS 0039-44	0039-44	0.436	...	...	...	...	...		...	MT
5C 31.00	0039+400	0.071	-23.01	...	24.02	...	...		...	Z
PKS 0043-424	0043-424	0.053	-21.80	...	26.27	...	...	IIg	...	Z
PKS 0043-42	0043-42	0.116	...	0.87	27.23	<23.58	34.00	II	<-2.70	MT
5C 31.75	0044+398	0.134	-22.37	...	24.46	...	...		...	Z
PKS 0045-25	0045-25	0.001	...	0.62	22.70	20.75	...	CH	-1.25	MT
3C 26	0051-038	0.210	-22.53	0.80	27.10	...	...		...	Z
3C 29	0055-01	0.045	-23.15	0.50	25.95	23.58	33.69	I	-1.65	Z,MC,B,MT
3C 28	0053+26	0.195	-22.96	1.06	27.15	<22.62	35.07	II	<-3.38	SKW,MC,G
B2 0055+26	0055+26	0.047	...	...	25.67	22.88	...		-1.97	G
B2 0055+30	0055+30	0.017	...	...	24.52	23.81	...		...	G
PKS 0057-180	0057-180	0.133	...	...	25.81	24.56	...	U	-0.38	C
PKS 0101+023	0101+023	0.390	-22.49	1.33	27.13	...	...	II	...	Z
3C 31	0104+32	0.016	-21.25	0.57	25.07	22.04	...	I	-2.20	S,G
3C 32	0105-16	0.400	...	1.10	28.28	<24.31	35.67	II	<-2.77	MT
3C 33	0106+69	0.060	-22.41	0.76	26.67	23.58	34.99	IIg	-2.25	Z,B,R,MC,G
3C 33.1	0106+72	0.181	...	0.62	27.13	24.37	35.36		-2.07	R,MC
3C 34.0	0107+31	0.689	...	0.06	28.41	<25.26	37.45	H	<-3.09	MC,G
PKS 0108-142	0108-142	0.052	...	...	24.96	23.09	...	Ig	-1.15	C
3C 35	0109+49	0.077	...	0.77	26.21	23.58	<33.61		-1.79	R
PKS 0114-476	0114-476	0.146	-23.54	...	26.86	...	...	II?	...	Z
PKS 0114-211	0114-211	0.075	...	...	25.82	23.09	...	U	...	C
PKS 0115-261	0115-261	0.053	...	...	24.92	23.35	...	I	-0.67	C
3C 36.0	0115+45	1.301	...	0.85	28.85	...	36.54	H	...	MC
B2 0116+31	0116+31	0.059	...	...	25.72	<25.34	...		<-0.00	G
3C 38	0117-15	0.565	...	0.90	28.52	...	36.48	II	...	MT
3C 40	0123-01	0.018	-22.06	0.90	25.27	23.90	33.61	I/II	-1.35	S,B,MC,MT
3C 41.0	0123+32	0.794	...	...	28.37	<25.88	...		<-1.66	G
3C 42	0125+28	0.395	-22.54	0.73	27.80	24.42	35.06	II	-2.58	Z,R,G
3C 44.0	0128+06	0.660	...	0.83	28.08	...	36.36	H	...	MC
PKS 0131-36	0131-36	0.030	...	0.51	25.76	24.18	33.06	II	-0.98	MT
3C 46	0132+37	0.438	...	1.13	27.75	24.47	36.23	II	-2.04	R,G
3C 49.0	0138+13	0.621	-23.80	0.65	28.16	25.38	36.60	H	-2.07	MC,G
NGC 708/B2	0149+35	0.016	-20.90	...	23.60	21.74	...		-1.00	S,G
3C 54.0	0152+43	0.827	...	0.82	28.37	...	36.57	H	...	MC
3C 55.0	0154+28	0.735	-24.60	1.04	28.61	<25.05	36.19	H	<-2.43	MC
B2 0206+35	0206+35	0.038	...	...	25.44	23.80	...		-0.75	G
PKS 0208-240	0208-240	0.231	...	...	26.20	<23.01	34.27	IIg	<-2.34	C
3C 61.1	0210+86	0.186	...	0.77	27.45	23.67	...		-2.91	R,G
3C 62	0213-13	0.148	-23.03	0.74	27.08	24.39	35.39	II	-1.87	S,MT
5C 6.1420	0213+33	0.448	-23.19	...	26.00	...	...	II	...	Z
PKS 0214-480	0214-480	0.064	-23.40	...	26.00	...	...	I	...	Z
PKS 0214-280	0214-280	0.220	-23.20	...	26.92	...	...		...	Z
3C 63	0218-02	0.175	-22.75	0.79	27.18	24.31	35.47	II	-1.96	Z,MC,B
3C 66B	0219+42	0.022	-23.20	0.62	25.63	23.56	...	I	-1.18	SKW,G
3C 65.0	0220+39	1.176	-25.30	0.75	29.00	24.87	36.27	H	-3.32	MC,G
3C 67	0221+27	0.310	-22.83	0.58	27.51	26.14	36.35	II	-0.67	Z,G,R
B2 0222+36	0222+36	0.033	...	...	24.19	23.81	...		...	G
PKS 0229-208	0229-208	0.090	...	...	25.46	23.01	33.41	U	...	C
PKS 0229+034	0229+034	0.273	-22.49	...	...	...	...	II	...	Z
3C 68.2	0231+31	1.575	...	...	28.62	<25.86	...		<-1.94	G
PKS 0235-19	0235-19	0.620	...	0.87	28.53	<23.73	36.54	II	<-3.86	MT
PKS 0240-217	0240-217	0.314	...	...	26.59	23.01	35.02		...	C
PKS 0240-00	0240-00	0.004	...	0.78	23.98	21.71	...		-1.40	MT
PKS 0247-207	0247-207	0.087	...	...	25.35	23.45	...	I	-0.97	C
PKS 0252-71	0252-71	0.566	...	1.14	28.82	...	...	U	...	MT
3C 75 N	0255+05	0.024	-22.88	0.80	25.58	22.98	32.63	I	-1.72	B,S
3C 75.0	0255+05	0.024	-22.75	0.80	25.56	22.96	32.64	I	-1.70	MC,MT
3C 75 S	0255+05	0.024	-22.86	0.80	25.56	22.65	32.63	I	-1.50	B,S
B2 0258+35	0258+35	0.016	...	...	24.63	<23.43	...		<-0.16	G
3C 76.1	0300+16	0.032	-21.93	0.77	25.45	22.66	...	I	-1.89	S,G
4C 39.11	0303+390	0.161	-23.75	0.96	26.78	...	...	II	...	Z
PKS 0304-122	0304-122	0.079	...	...	25.43	23.45	<33.06	I?	...	C
3C 78	0305+03	0.029	-23.49	0.50	25.68	24.48	34.02	I	-0.51	S,B,MC,MT
3C 79	0307+16	0.256	-22.60	0.92	27.68	24.55	36.68	II	-2.15	S,MC,G,R
PKS 0307-305	0307-305	0.068	...	...	25.15	23.45	...	IIg	...	C
3C 83.1B	0314+41	0.025	-23.55	0.64	25.43	...	...	I	...	SKW

TABLE 11—*Continued*

Name (1)	IAU (2)	redshift (3)	Magnitude (4)	α (5)	P_{total} (6)	P_{core} (7)	Line-Lum (8)	FR (9)	$R=P_l/P_c$ (10)	Reference (11)
3C 84	0316+41	0.018	-24.11	0.78	25.60	...	35.21	I	...	S,GG
ForA/NGC 1316	0320-37	0.005	-23.21	0.52	25.46	21.45	<32.84	I	-3.44	MT,SP
3C 88.0	0325+02	0.030	-22.57	0.60	25.58	23.81	34.05	I/II	-1.08	S,B,MC,MT
PKS 0326-288	0326-288	0.108	...	...	25.66	23.52	35.16	II	-1.35	C
B2 0326+39	0326+39	0.024	...	...	24.68	23.25	...		-0.50	G
3C 89	0331-01	0.139	-23.25	0.98	26.94	24.53	34.68	I	-1.30	Z,MC,Z
B2 0331+39	0331+39	0.020	...	...	24.48	23.42	...		0.12	G
NGC 1399	0336-35	...	-22.48	...	23.52	22.92	32.38	I?	...	GG,SP
NGC 1404	0336-35	...	-22.50	...	<20.92	20.62	<32.08	I?	...	SP,GG
PKS 0337-216	0337-216	0.414	-22.62	...	27.17	...	...		...	Z
NGC 1427	0340-35	...	-21.31	...	<20.72	20.42	<31.61	I?	...	SP,GG
PKS 0344-345	0344-345	0.054	...	...	25.40	23.22	33.86	Ig	-1.26	C
PKS 0349-278	0349-278	0.066	-22.50	0.72	26.48	23.42	34.39	IId	-2.20	Z,B,C,MT
3C 98	0356+10	0.031	-21.95	0.70	26.02	22.56	34.17	IId	-2.74	Z,G,MC,R,B
3C 105.0	0404+03	0.089	-20.83	0.60	26.56	23.68	34.17	II	-2.24	B,MT,Z
3C 103.0	0404+42	0.331	...	0.79	27.92	...	34.81		...	MC
PKS 0409-75	0409-75	0.693	...	0.86	29.11	...	35.33	II	...	MT
3C 107.0	0409-01	0.785	-23.80	1.02	28.38	...	37.15	H	...	MC
3C 109.0	0410+11	0.306	-24.04	0.85	27.74	26.21	36.41	II	-0.58	MC,Z,B,R
4C 14.11	0411+14	0.207	...	0.84	27.12	24.72	34.61		-1.47	R
NGC 1549	0414-55	...	-21.66	...	...	...	<32.31	I?	...	GG
3C 114.0	0417+17	0.815	...	0.89	28.22	...	35.86	H	...	MC
PKS 0424-268	0424-268	0.091	...	...	25.46	23.58	...	U	-0.99	C
PKS 0427-53	0427-53	0.038	-23.61	0.20	25.55	23.55	<33.32	I?	-1.77	MT,N
3C 120	0430+05	0.033	-22.45	...	25.36	25.19	...	I	-1.17	S,MT
3C 123	0433+29	0.218	...	0.70	28.44	26.45	34.86		-1.22	RG
PKS 0434-225	0434-225	0.069	...	...	25.20	21.58	...	Ig	-2.75	C
3C 124.0	0439+01	1.083	...	1.18	28.72	...	37.36	H	...	MC
PKS 0442-28	0442-28	0.147	...	0.93	27.38	...	35.11	II	...	MT
PKS 0449-175	0449-175	0.031	...	...	24.34	21.58	32.67	I	...	C
B2 0453-20	0453-20	0.035	...	0.73	25.79	23.33	<33.42	I?	-1.65	MT
3C 132	0453+22	0.214	...	0.68	27.28	<24.75	...		<-1.78	R
PKS 0453-206	0453-206	0.035	...	...	25.22	22.53	33.26	I?	-1.86	C
4C -04.17	0456-043	0.118	-22.99	...	26.12	...	...		...	Z
PKS 0456-301	0456-301	0.131	...	...	26.14	<22.16	...	U	<-3.11	C
3C 133.0	0459+25	0.278	...	0.70	27.70	...	34.65		...	MC
PKS 0502-103	0502-103	0.041	...	...	24.82	22.16	...		...	C
PKS 0511-305	0511-305	0.058	...	...	25.39	22.57	33.64	IIg	-1.88	C
3C 135	0511+00	0.127	-22.47	0.92	26.80	23.51	...	II	...	Z,R
PKS 0518-458	0518-458	0.035	-21.21	1.07	26.86	24.74	34.58	IId	-1.16	Z,MT
PKS 0521-365	0521-365	0.061	-23.03	...	26.64	...	...		...	Z
PKS 0521-36	0521-36	0.055	...	0.49	26.63	25.27	...		-0.75	MT
PKS 0521-329	0521-329	0.210	...	...	26.23	<24.05	<33.38	T	<-1.13	C
PKS 0523-327	0523-327	0.076	...	...	25.30	24.05	...	II	...	C
3C 142.1	0528+06	0.406	...	0.89	27.49	...	36.22		...	MC
PKS 0533-120	0533-120	0.157	...	...	26.06	24.75	<33.49	I?	-0.53	C
PKS 0545-199	0545-199	0.053	...	...	24.83	23.23	...	I	-0.89	C
PKS 0546-329	0546-329	0.037	...	...	24.73	23.23	...	I?	...	C
PKS 0548-317	0548-317	0.033	...	...	24.53	23.23	...	II	...	C
PKS 0600-131	0600-131	0.150	...	...	25.91	22.51	...	II	-2.50	C
PKS 0611-254	0611-254	0.133	...	...	25.76	24.13	...	I?	-0.82	C
PKS 0614-349	0614-349	0.329	...	...	27.01	26.28	35.42	U	-0.02	C
PKS 0620-52	0620-52	0.051	...	0.87	26.11	24.48	<33.69	I	-0.58	MT
PKS 0634-206	0634-206	0.056	-23.82	0.80	26.48	23.29	35.04	II	-2.32	B
PKS 0634-205	0634-205	0.055	-22.48	...	25.72	22.74	34.10	I	-2.16	C,S
3C 165.0	0640+23	0.296	-25.00	0.71	27.54	...	35.04		...	MC
3C 169.1	0647+45	0.633	...	0.90	27.99	...	36.67	H	...	MC
B2 0648+27	0648+27	0.041	...	...	24.28	24.18	35.35		...	M,G
3C 171	0651+54	0.238	-21.52	0.87	27.39	23.71	36.17	II	-2.71	S,G,N,MC
3C 172.0	0659+25	0.519	...	0.86	28.11	...	36.61	H	...	MC
3C 173.1	0702+74	0.292	...	0.88	27.58	24.54	34.76		-2.08	R,G
B2 0708+32	0708+32	0.067	...	...	24.74	23.46	...		-0.29	G
3C 175.1	0711+14	0.920	...	0.84	28.60	...	36.53	H	...	MC
PKS 0718-340	0718-340	0.030	...	...	24.71	22.74	...	II?	...	C
PKS 0719-553	0719-553	0.216	-23.18	...	27.12	...	...		...	Z
PKS 0719-119	0719-119	0.091	...	...	25.56	22.74	...	U	...	C
B2 0722+30	0722+30	0.019	...	...	23.77	22.90	34.32	I	0.86	M,G
3C 180.0	0724-01	0.220	...	0.84	27.27	...	35.45		...	MC
3C 184.0	0733+70	0.994	-25.70	0.68	28.75	25.88	36.76	H	-2.13	MC,G
3C 184.1	0734+80•	0.118	-22.20	0.68	26.68	23.58	35.82	II	-2.40	Z,G,R
PKS 0745-191	0745-191	0.103	...	1.05	26.66	24.92	35.69	AM	-0.47	B,C
DA 240	0745+56	0.035	...	0.77	25.82	23.99	33.04		-0.95	R
B2 0755+37	0755+37	0.041	...	...	25.63	24.15	33.70		-0.56	M,G
B2 0800+24	0800+24	0.043	...	...	24.41	22.38	<33.45	I	-1.18	M,G

TABLE 11—*Continued*

Name (1)	IAU (2)	redshift (3)	Magnitude (4)	α (5)	P_{total} (6)	P_{core} (7)	Line-Lum (8)	FR (9)	$R=P_l/P_c$ (10)	Reference (11)
3C 192.0	0802+24	0.060	-21.94	0.79	26.24	23.04	34.71	IId	-2.44	S,B,R,G,MC
3C 195	0806-10	0.110	...	0.72	26.75	24.49	35.98	II	-1.46	MT
PKS 0806-103	0806-103	0.133	...	...	26.33	23.63	...	IIg	-1.88	C
3C 196.1	0812-02	0.198	-23.32	0.73	27.18	24.99	33.06	AM	-1.32	S,Z,B,MC
3C 198	0819+06	0.082	-21.70	0.80	26.23	...	...	IIn	...	Z
B2 0822+34	0822+34	0.406	-22.33	...	27.18	...	...	II	...	Z
3C 200	0824+29	0.458	-22.56	0.84	27.89	25.69	...	IId	-1.29	HL,G,R
B2 0828+32AB	0828+32	0.051	...	...	25.68	22.56	...		-2.30	G
55W010	0832+45	0.452	-23.13	...	26.00	...	...	C	...	HL
55W016	0833+45	0.375	-22.04	...	25.11	...	...	I?	...	HL
55W023	0833+45	0.360	-22.61	...	24.90	...	...	I?	...	HL
4C 14.27	0832+14	0.392	...	1.15	27.63	<23.84	...		<-2.54	R
B2 0835+37	0835+37	0.396	-22.00	...	26.68	...	...	C	...	HL
B2 0836+29(II)	0836+29	0.079	...	...	25.68	24.54	35.14	II	-0.04	M,G
55W097	0838+44	0.365	-21.31	...	24.30	...	...	I?	...	HL
B2 0838+32	0838+32	0.068	...	...	25.58	<24.33	...		<-0.23	G
0841+42	0841+42	0.425	...	...	24.00	...	...	I?	...	HL
55W150	0842+45	0.465	-21.45	...	24.48	...	...	I?	...	HL
55W161	0843+44	0.402	-21.91	...	24.48	...	...	I?	...	HL
B2 0844+31	0844+31	0.068	...	...	25.86	24.05	...		-0.95	G
65W090	0846+46	0.500	...	...	23.81	...	...	I?	...	BRE
65W258	0846+46	0.500	...	...	23.76	...	...	I?	...	BRE
65W065	0846+45	0.222	-23.90	...	23.82	...	...	I?	...	BRE
65W117	0846+45	0.440	-22.10	...	24.64	...	...	I?	...	BRE
65W186B	0846+46	0.500	-22.00	...	25.69	...	...	I?	...	BRE
B2 0847+37	0847+37	0.407	-22.75	0.60	27.03	...	...	IId	...	Z
C028	0852+17	0.440	...	...	23.66	...	...	I?	...	BRE
C036	0852+17	0.400	...	...	24.39	...	...	I?	...	BRE
C089	0852+17	0.203	-22.20	...	23.35	...	...	I?	...	BRE
C084	0852+17	0.327	-21.70	...	25.25	...	...	I?	...	BRE
3C 210.0	0855+28	1.169	...	0.78	28.79	...	36.77	H	...	MC
PKS 0859-25	0859-25	0.305	...	0.60	27.48	...	...	U	...	MT
3C 217.0	0905+38	0.897	-24.50	0.77	28.57	<26.20	36.19	H	<-1.53	MC,G
B2 0908+37	0908+37	0.104	...	...	25.73	24.04	...		-0.82	G
B2 0913+38	0913+38	0.071	...	...	26.24	<22.33	...		<-3.10	G
3C 218	0915-118	0.065	-23.46	0.90	27.33	24.51	34.58	I	-1.84	Z,B,MT
PKS 0915-118	0915-118	0.053	...	...	26.54	23.63	34.12	Ig	...	C
B2 0915+32	0915+32	0.062	...	...	24.88	23.12	34.74	I	-0.90	M,G
3C 219	0917+45	0.174	-23.21	0.81	27.51	24.88	35.44	II	-1.80	S,G,MC,R,B
PKS 0921-213	0921-213	0.053	...	...	24.73	23.63	...		...	C
B2 0922+36B	0922+36	0.112	...	...	25.99	23.90	...		-1.24	G
B2 0924+30	0924+30	0.027	...	...	24.72	<20.78	<33.53		<-3.13	M,G
3C 220.1	0926+79	0.610	...	...	28.03	25.57	...		-1.63	G
3C 220.3	0931+83	0.680	...	...	28.29	<25.57	...		<-1.89	G
3C 223	0936+07	0.137	-22.58	0.74	26.85	23.90	33.35	II	-1.90	Z,G,B,R,MC
3C 223.1	0938+39	0.108	-22.67	0.56	26.31	...	...	II	...	Z
3C 225.2	0939+13	0.582	...	0.94	28.36	24.37	36.47	H	-2.97	MC,G
3C 226.0	0941+10	0.818	-26.50	0.88	28.58	25.60	36.60	H	-2.02	MC,G
3C 227	0945+07	0.086	-22.20	0.80	26.77	23.80	35.62	IIg	-1.90	G,B,MC,MT
4C 73.08	0945+73	0.059	...	0.85	26.08	23.47	34.45		-1.67	R
3C 228.0	0947+14	0.552	...	1.00	28.31	25.45	37.04	H	-1.76	MC,G
3C 234	0958+29	0.185	-23.61	0.86	27.46	25.22	36.73	II	-1.16	S,G,R
4C 20.20	1000+201	0.168	-23.49	...	26.56	...	...	I	...	Z
B2 1003+26	1003+26	0.116	...	...	25.23	22.71	...		-1.70	G
3C 236	1003+35	0.099	-22.80	0.51	26.62	24.83	34.51	IId	-0.90	Z,R,G
NGC 3136	1004-67	...	...	...	<22.12	21.82	33.43	I?	...	SP,GG
3C 237.0	1005+07	0.877	...	0.51	28.84	...	37.14	H	...	MC
B2 1005+28	1005+28	0.148	...	...	25.36	23.24	...		-1.28	G
4C 14.36	1007+142	0.215	-22.84	...	26.72	...	...		...	Z
3C 239.0	1008+46	1.781	...	...	29.01	24.83	...		-3.37	G
3C 241.0	1019+22	1.617	...	...	28.84	25.52	...		-2.50	G
NGC 3250	1024-39	...	-22.89	...	<21.22	20.92	<32.80	I?	...	SP,GG
B2 1025+39	1025+39	0.360	-23.07	0.60	27.81	...	...	II	...	Z
3C 244.1	1030+58	0.428	-22.93	0.82	28.05	<23.82	36.28	II	<-3.34	MC,G,R,HL
B2 1037+30	1037+30	0.091	...	...	25.60	<24.47	...		<-0.04	G
B2 1040+31	1040+31	0.036	...	...	24.97	23.48	33.56	I	-0.57	M,G
PKS 1053-282	1053-282	0.061	...	...	25.30	23.63	33.91	II	...	C
3C 109.0	1054+11	0.036	...	...	25.86	24.15	...		-0.83	G
3C 247.0	1056+43	0.735	-20.60	0.61	28.35	25.09	36.84	H	-2.60	MC,G
B2 1101+38	1101+38	0.030	...	...	24.65	24.39	33.80		...	M,G
B2 1102+30	1102+30	0.072	...	...	25.32	23.76	...		-0.67	G
PKS 1103-244	1103-244	0.234	...	...	26.36	24.71	<33.87	I?	-0.71	C
NGC 3557	1104-36	...	-23.46	...	23.82	23.52	33.36	I?	...	GG,SP
4C 37.29A	1107+379	0.346	-22.59	...	27.48	...	...	II	...	Z

TABLE 11—*Continued*

Name (1)	IAU (2)	redshift (3)	Magnitude (4)	α (5)	P_{total} (6)	P_{core} (7)	Line-Lum (8)	FR (9)	$R=P_l/P_c$ (10)	Reference (11)
3C 252.0	1108+35	1.104	-25.50	0.88	28.79	25.10	37.19	H	-2.73	MC,G
B2 1108+27	1108+27	0.033	...	...	...	...	33.48	I	...	M
B2 1113+24	1113+24	0.102	...	...	25.06	<22.12	...		<-2.12	G
B2 1113+29	1113+29	0.049	...	...	25.70	23.62	33.87	II	-1.24	M,G
B2 1116+28	1116+28	0.067	...	...	25.30	23.75	...		-0.65	G
PKS 0116-190	1116-190	0.280	...	...	26.50	25.09	34.58	U	-0.56	C
3C 258	1122+19	0.165	-20.75	1.30	26.27	...	...		...	Z
4C 20.25	1123+203	0.132	-23.82	1.30	25.99	...	...	II	...	Z
B2 1122+39	1122+39	0.007	...	...	23.98	21.06	33.41	I	-2.10	M,G
NGC 3706	1127-36	...	-22.61	...	22.62	22.32	<31.67	I?	...	SP,GG
4C 01.31	1134+015	0.430	-23.52	0.75	27.57	...	...	II	...	Z
3C 263.0	1137+66	0.656	...	0.82	28.36	...	35.77	H	...	MC
3C 263.1	1140+22	0.824	-22.80	0.87	28.68	<27.21	36.83	H	<-0.37	MC
B2 1141+37	1141+37	0.115	...	...	26.46	23.37	...		-2.27	G
3C 264.0	1142+19	0.021	-23.23	0.75	25.51	23.58	33.39	I	-0.98	S,MC,B,G
3C 265.0	1142+31	0.811	-25.00	0.96	28.68	<25.91	37.71	H	<-1.72	MC,LRL,G
3C 266.0	1143+50	1.275	-26.30	1.01	28.96	<25.05	37.50	H	<-2.80	MC,G
B2 1144+35	1144+35	0.063	...	...	24.74	24.62	34.41	I	...	M,G
3C 267.0	1147+13	1.140	-25.20	0.93	28.95	25.59	36.84	H	-2.34	MC,G
4C 29.44	1152+30	0.329	-23.06	...	27.53	...	...	II	...	Z
3C 268.1	1157+73	0.974	-24.90	0.59	28.95	25.14	36.14	H	-3.17	MC,G
B2 1201+39	1201+39	0.445	-22.52	0.41	27.07	...	...	IIg	...	Z
3C 268.3	1203+64	0.371	-21.48	0.50	27.70	<25.89	35.78	II	<-1.16	MC,HL,R,G
B2 1204+34	1204+34	0.079	...	...	25.42	23.78	...		-0.76	G
B2 1204+24	1204+24	0.077	...	...	24.83	23.30	...		-0.62	G
PKS 1214+038	1214+038	0.077	-22.98	...	25.90	...	...	I?	...	Z
PKS 1215+039	1215+039	0.076	-23.23	...	26.26	...	...	II?	...	Z
PKS 1216-100	1216-100	0.087	-23.56	...	26.43	...	...	I?	...	Z
3C 270	1216+06	0.006	-22.65	0.56	24.80	22.68	<32.46	I	-1.46	MT,SKW,GG
B2 1217+29	1217+29	0.002	...	...	22.04	21.82	33.12		...	M,G
NGC 4373	1222-39	...	-23.22	...	22.62	22.32	<31.80	I?	...	SP,GG
3C 272.1	1222+13	0.004	-22.19	0.60	23.80	21.92	32.67	I	-1.47	G,SKW,B,GG
3C 274.0	1228+12	0.004	-22.00	0.76	25.65	23.37	33.77	I	-1.47	MC,G,B,SKW
3C 274.1	1232+21	0.422	-22.42	0.87	27.98	25.03	...	IIg	-1.99	HL,R,G
3C 275.0	1239-04	0.480	-22.76	0.90	28.04	...	36.30	II	...	MC,B,HL
B2 1243+26B	1243+26	0.089	...	...	25.47	<22.78	...		<-1.87	G
NGC 4696	1244-41	...	-23.33	...	24.59	...	33.62	I?	...	GG
NGC 4696B	1244-40	...	-23.45	...	23.52	23.22	32.50	I?	...	SP
PKS 1246-41	1246-41	0.009	...	0.76	24.77	...	...	U	...	MT
B2 1245+34	1245+34	0.409	-22.50	...	27.01	...	...	IIg	...	Z
3C 278	1251-12	0.014	-20.73	0.60	25.12	22.87	33.37	I	-1.55	S,B,MC,MT
3C 277.2	1251+15	0.766	-25.00	1.02	28.40	<25.86	37.07	H	<-1.41	MC,G
3C 277.3	1251+27	0.086	-22.55	0.58	26.27	...	...	II	...	Z
B2 1254+27	1254+27	0.025	-22.85	...	...	...	33.67	I	...	M,N
3C 280.0	1254+47	0.998	-25.00	0.81	29.01	24.93	37.55	H	-3.20	MC,G
PKS 1254-300	1254-300	0.054	...	...	25.03	<21.99	...	II	<-2.09	C
5C 12.71	1255+35	0.436	-22.21	...	25.75	...	...	I	...	HL
B2 1256+28	1256+28	0.022	...	...	24.50	21.63	<32.87		-2.04	M,G
5C 12.91	1256+37	0.464	-22.99	...	25.96	...	...	IIn	...	HL
PKS 1258-229	1258-229	0.130	...	...	25.68	24.34	34.60	II	-0.56	C
5C 12.168	1259+37	0.424	-22.80	...	25.77	...	...	I	...	HL
M001	1300+30	0.168	-22.00	...	23.94	...	...	I?	...	BRE
M006B	1300+30	0.167	-21.40	...	24.19	...	...	I?	...	BRE
M009	1300+30	0.500	...	...	24.53	...	...	I?	...	BRE
M025	1300+30	0.293	-21.80	...	23.67	...	...	I?	...	BRE
M029	1300+30	0.500	...	...	24.59	...	...	I?	...	BRE
M111	1300+30	0.200	-22.10	...	23.56	...	...	I?	...	BRE
M113	1300+30	0.388	-21.80	...	24.45	...	...	I?	...	BRE
5C 12.217	1301+34	0.428	-22.06	...	26.08	...	...	IIg	...	HL
5C 12.241	1302+36	0.487	-22.15	...	26.89	...	...	IId	...	HL
5C 12.264	1303+35	0.373	-22.84	...	26.00	...	...	C	...	HL
5C 12.251	1303+369	0.312	-23.06	...	27.36	...	...	D	...	Z
PKS 1306-09	1306-09	0.464	...	0.65	28.08	...	...	U	...	MT
5C 12.304	1307+34	0.460	-22.31	...	26.38	...	...	C	...	HL
3C 284.0	1308+27	0.235	...	0.90	27.18	23.60	35.60	II	-2.21	G,MC,R
B2 1316+29	1316+29	0.073	...	...	25.85	23.84	...		-1.16	G
B2 1317+33	1317+33	0.038	...	...	...	...	33.65	I	...	M
NGC 5090A	1318-43	0.011	-22.16	0.96	25.01	23.48	<32.63	I	-0.30	MT,SP
B2 1318+34	1318+34	0.023	...	...	...	...	34.26		...	M
3C 285	1319+42	0.079	-22.46	0.95	26.15	23.25	34.75	IIn	-2.10	S,MC,B,R,G
B2 1321+31	1321+31	0.016	...	...	24.60	22.37	<33.29		-1.40	M,G
CenA	1322-42	0.002	...	0.79	23.80	21.62	...	T	-1.31	MT
B2 1322+36	1322+36	0.018	...	...	24.35	23.29	33.03	I	0.13	M,G
PKS 1323-271	1323-271	0.043	...	...	24.99	22.47	31.96	U	-1.55	C

TABLE 11—*Continued*

Name (1)	IAU (2)	redshift (3)	Magnitude (4)	α (5)	P_{total} (6)	P_{core} (7)	Line-Lum (8)	FR (9)	$R=P_l/P_c$ (10)	Reference (11)
PKS 1324-300	1324-300	0.200	...	...	26.13	23.36	35.35	IIg	-1.86	C
PKS 1329-328	1329-328	0.048	...	...	24.70	21.97	...	II?	...	C
PKS 1329-257	1329-257	0.194	...	...	26.19	24.76	...	II	-0.59	C
3C 287.1	1330+02	0.216	-22.69	0.52	27.08	...	...	II	...	Z
PKS 1331-099	1331-099	0.081	-22.78	...	26.26	...	...	I?	...	Z
PKS 1333-33	1333-33	0.013	-23.73	...	25.06	24.52	32.92	I?	...	SP,GG,MT
3C 288.0	1336+39	0.246	...	...	27.37	24.87	...		-1.67	G
B2 1339+26	1339+26	0.072	...	...	25.44	24.08	...		-0.40	G
4C 05.57	1340+053	0.133	-22.89	...	26.56	...	...	II?	...	Z
B2 1340+28	1340+28	0.126	...	...	25.41	23.37	...		-1.19	G
3C 289.0	1343+50	0.967	-23.80	0.81	28.68	<24.59	36.11	H	<-3.21	MC,G
4C 12.50	1345+123	0.122	-23.55	...	26.72	...	...		...	Z
B2 1346+26	1346+26	0.063	-24.12	...	25.73	23.95	35.13	I	-0.91	M,G,N
B2 1347+28	1347+28	0.072	...	...	25.06	23.03	...		-1.19	G
3C 292.0	1349+64	0.710	...	...	28.06	<24.91	...		<-2.34	G
3C 293	1350+31	0.045	-22.84	0.45	25.96	23.94	34.84	II	-1.16	S,G,M
B2 1357+28	1357+28	0.063	...	...	25.06	23.02	...		-1.20	G
PKS 1358-113	1358-113	0.037	...	...	24.89	23.11	...		-0.72	C
PKS 1358+125	1358+125	0.025	-22.71	...	25.20	...	32.78	II	...	S,B
B2 1358+30	1358+30	0.110	...	...	25.65	<22.31	...		<-2.52	G
4C 62.22	1358+62	0.429	-21.96	...	27.62	...	...	U	...	Z
PKS 1405-298	1405-298	0.087	...	...	25.26	24.06	...	U	-0.51	C
3C 295.0	1409+52	0.461	-23.99	0.63	28.78	25.15	35.43	II	-2.73	MC,B,R,HL,G
PKS 1414-212	1414-212	0.110	...	...	25.63	22.41	<32.56	T	-2.30	C
3C 296.0	1414+11	0.024	-23.79	0.67	25.36	23.27	...	I	-1.10	S,G
PKS 1417-192	1417-192	0.119	-23.59	...	26.45	22.41	...	II	...	Z,C
3C 299.0	1419+41	0.367	-22.81	0.65	27.70	25.56	36.52	II	-1.41	MC,R,G,Z
3C 300	1420+19	0.270	-21.90	0.75	27.58	24.43	36.15	II	-2.21	S,MC,G,R
B2 1422+26	1422+26	0.037	...	...	25.07	23.16	33.84	I	-1.05	M
PKS 1423-177	1423-177	0.107	...	...	25.63	23.01	34.20	II	-1.72	C
3C 300.1	1425-01	1.170	-23.60	0.68	28.97	...	36.64	H	...	MC
B2 1430+25	1430+25	0.018	...	...	24.30	<21.16	...		<-2.32	G
B2 1441+26	1441+26	0.062	...	...	25.03	<22.06	...		<-2.16	G
3C 303	1441+52	0.141	-22.43	0.76	26.76	25.13	35.17	II	-0.73	Z,G,R
3C 303.1	1443+77	0.267	-22.70	0.76	27.35	<24.27	36.11		<-2.25	MC,G
B2 1447+27	1447+27	0.031	...	...	24.13	23.12	...		0.24	G
3C 305.1	1447+77	1.132	-23.30	0.85	28.97	...	37.41	H	...	MC
3C 305	1448+63	0.041	-23.17	0.85	25.84	23.00	33.41	II	-1.77	S,B,G
PKS 1449-129	1449-129	0.070	...	...	25.26	22.37	<32.15	I?	-2.05	C
3C 306.1	1452-04	0.441	-22.88	0.90	27.89	...	36.24	II	...	MC,Z
NGC 5813	1458+01	...	-21.87	...	22.04	...	33.15	I?	...	GG
3C 310	1502+26	0.054	-22.10	0.92	26.46	24.00	...	IIn	-1.64	Z,G
3C 313	1508+08	0.461	-22.61	0.82	28.13	<23.96	36.56	II	<-3.06	B,MC,Z
3C 315	1511+26	0.108	-22.42	0.72	26.68	<24.87	...	I	<-0.95	Z,G
B2 1512+30	1512+30	0.093	...	...	24.99	<22.16	...		<-2.01	G
3C 317	1514+07	0.035	-23.13	1.02	26.10	24.50	34.94	I	-0.26	Z,MC,B,MT
PKS 1517-283	1517-283	0.123	...	...	25.70	23.59	...	Ig	-1.20	C
3C 318.0	1517+20	0.752	...	...	28.26	<26.31	...		<-1.10	G
3C 318.1	1519+07	0.046	-21.56	1.93	25.09	...	...		...	SKW
B2 1521+28	1521+28	0.083	...	...	25.65	24.30	...		-0.38	G
3C 319	1522+54	0.192	...	0.90	27.17	<23.27	<34.28		<-2.92	R
B2 1525+29	1525+29	0.065	...	...	24.89	22.66	<34.09	I	-1.40	M,G
B2 1527+30	1527+30	0.114	...	...	25.39	23.33	...		-1.22	G
B2 1528+29	1528+29	0.084	...	...	25.34	23.13	...		-1.38	G
3C 321	1529+24	0.096	-23.37	0.60	26.54	24.10	35.72	II	-1.78	Z,MC,R,B,G
3C 323.0	1529+24	0.679	...	0.81	28.14	...	35.68	H	...	MC
3C 320	1529+35	0.342	-23.15	0.75	27.51	...	...	II	...	Z
4C 34.42	1539+34	0.402	-23.17	0.61	27.85	...	...	II	...	Z
3C 324.0	1547+21	1.206	-26.60	0.90	29.05	<24.87	37.55	H	<-3.20	MC,G
PKS 1547-79	1547-79	0.483	...	0.85	28.23	<24.64	36.55	II	<-2.66	MT
3C 325.0	1549+62	0.860	...	...	28.48	24.56	...		-3.10	G
3C 326	1549+20	0.089	...	0.88	26.50	23.66	<33.57	II	-2.00	R,G,Z
PKS 1549-79	1549-79	0.150	...	0.17	26.83	...	...	U	...	MT
B2 1553+24	1553+24	0.043	-23.00	...	...	...	33.35	I	...	M,N
PKS 1553-328	1553-328	0.065	...	...	25.07	23.78	33.25	I	-0.60	C
PKS 1555-140	1555-140	0.096	...	...	25.24	24.75	34.21		-0.20	C
B2 1557+26	1557+26	0.044	...	...	24.32	23.41	...		0.64	G
3C 327.0	1559+02	0.104	-23.57	0.61	27.00	24.20	34.27	II	-1.80	S,B,MT
3C 327.1	1602+01	0.463	...	0.61	28.41	25.97	35.84	II	-1.21	MC,MT
NGC 6047	1602+17	0.032	-22.55	...	...	...	...	I	...	S
3C 327.1	1602+01	0.031	...	1.02	25.78	23.43	<32.91	II	-1.21	B
B2 1603+32	1603+32	0.374	-22.68	0.70	26.51	...	...		...	Z
3C 330.0	1609+66	0.550	-24.10	0.71	28.46	<25.46	37.04	H	<-2.22	MC,G
B2 1610+29	1610+29	0.031	-23.52	...	24.13	<22.40	<32.83	I	<-0.85	M,G,N

TABLE 11—*Continued*

Name (1)	IAU (2)	redshift (3)	Magnitude (4)	α (5)	P_{total} (6)	P_{core} (7)	Line-Lum (8)	FR (9)	$R=P_l/P_c$ (10)	Reference (11)
B2 1613+27	1613+27	0.065	...	...	24.90	23.65	...		-0.24	G
3C 332	1615+32	0.152	-22.95	0.61	26.69	23.98	...	II	-1.89	Z,G
B2 1615+35	1615+35	0.030	...	...	25.31	23.02	33.95	II	-1.45	M,G
B2 1621+38	1621+38	0.031	-23.74	...	24.58	23.31	33.66	I	-0.26	M,G,N
3C 341.0	1626+27	0.448	-22.26	0.85	27.81	24.05	35.92	II	-2.80	MC,R,G,Z
3C 338	1626+39	0.030	-24.00	1.19	25.87	23.61	34.08	I	-1.40	S,M,G
3C 340.0	1627+23	0.775	-24.20	0.73	28.38	<24.33	36.52	H	<-3.25	MC,G
3C 337.0	1627+44	0.635	-24.00	0.63	28.24	<24.10	36.49	H	<-3.46	MC,G
B2 1637+29	1637+29	0.087	...	...	25.42	23.62	...		-0.93	G
3C 343.1	1637+62	0.750	...	0.32	28.44	<26.80	36.30	H	<-1.27	MC,G
B2 1638+32	1638+32	0.140	...	...	25.69	24.72	...		0.37	G
3C 346	1641+17	0.161	-23.39	0.80	27.03	25.43	35.35	II	-0.63	Z,MC,B,G
B2 1643+27	1643+27	0.102	...	...	25.10	23.25	...		-0.99	G
4C 17.71	1645+17	0.314	-22.85	0.60	27.29	...	...		...	Z
3C 348	1648+05	0.154	-23.27	1.00	28.26	24.08	...	I	-3.10	Z,MT
B2 1652+39	1652+39	0.034	...	...	24.93	24.78	34.69		...	M,G
PKS 1654-137	1654-137	0.101	...	...	25.74	22.99	<32.23	II	-1.79	C
B2 1658+30	1658+30	0.035	...	...	24.91	23.64	...		-0.26	G
B2 1657+32A	1657+32	0.063	...	...	25.32	22.63	...		-1.88	G
B2 1658+32A	1658+32	0.102	...	...	25.42	23.02	...		-1.57	G
PKS 1712-120	1712-120	0.058	...	...	24.98	23.03	<32.35	Ig	-1.12	C
53W032	1715+49	0.370	-22.98	...	25.30	...	...	I?	...	HL
53W039	1715+50	0.402	-22.86	...	24.90	...	...	I?	...	HL
3C 352.0	1717-00	0.806	...	1.03	28.42	...	36.91	H	...	MC
3C 353	1717-00	0.030	-20.65	0.71	26.70	23.85	33.84	I/II	-1.85	Z,MC,B
53W076	1719+49	0.390	-22.53	...	24.60	...	...	C	...	HL
3C 356.0	1723+51	1.079	-26.10	1.02	28.77	25.04	37.47	H	-2.62	MC,G
3C 357	1726+31	0.167	...	...	26.85	23.82	...		-2.21	G
PKS 1733-56	1733-56	0.098	...	0.73	26.97	25.48	35.01	II	-0.60	MT
B2 1736+32	1736+32	0.074	...	...	25.14	23.27	...		-1.02	G
B2 1752+32B	1752+32	0.045	...	...	24.44	23.01	...		-0.49	G
3C 368.0	1802+11	1.132	-26.60	1.24	28.90	<24.99	37.65	H	<-2.56	MC,G
3C 371	1807+69	0.050	-23.24	0.30	25.57	...	...	C	...	S
PKS 1814-36	1814-36	0.063	...	0.92	26.90	...	...	U	...	MT
B2 1827+32A	1827+32	0.066	...	...	25.13	23.68	...		-0.52	G
3C 381	1832+47	0.161	-22.83	0.81	27.03	23.82	34.96	II	-2.47	Z,G,R
3C 382	1833+32	0.058	-23.67	0.59	26.30	24.44	33.38	II	-1.10	S,M,MC,R
3C 386	1836+17	0.018	-22.55	0.59	25.30	...	...	I	...	LRL
PKS 1839-48	1839-48	0.112	...	0.75	26.69	24.98	<33.46	I	-0.84	MT
3C 388	1842+30	0.091	-24.07	0.70	26.70	24.36	33.92	IIn	-1.58	S,G,R
3C 390.3	1845+79	0.056	-22.35	0.75	26.56	24.69	35.87	IId	-1.06	Z,B,G,R
B2 1855+37	1855+37	0.055	-24.98	...	25.02	<24.11	<33.48	I	< 0.65	M,G
PKS 1928-340	1928-340	0.098	-23.63	...	26.21	...	...	I?	...	Z
PKS 1932-46	1932-46	0.231	...	1.03	28.12	<25.24	35.62	II?	<-1.75	MT
PKS 1934-638	1934-638	0.182	-22.38	0.88	26.92	...	...	U	...	Z,MT
PKS 1938-15	1938-15	0.452	...	0.82	28.35	...	...		...	MT
3C 401	1939+60	0.201	...	0.71	27.40	24.84	34.72		-1.78	R
3C 402	1940+50	0.025	-21.86	0.68	25.23	...	...		...	SKW
3C 403.0	1949+02	0.059	-22.35	0.45	26.33	23.18	35.00	II	-2.29	S,B,MC,MT
PKS 1954-55	1954-55	0.060	...	0.78	26.42	23.91	<33.12	I	-1.66	MT
3C 405	1957+40	0.057	-23.02	0.74	25.76	24.65	35.37	II	-3.37	S,B
PKS 2013-308	2013-308	0.089	...	...	25.33	23.03	32.27	I	...	C
PKS 2030-230	2030-230	0.132	-22.20	...	26.70	23.03	35.14	II?	...	Z,C
PKS 2040-267	2040-267	0.038	...	...	24.98	22.26	...	IIg	-1.90	C
3C 424	2045+06	0.127	-21.88	0.85	26.75	...	...	I	...	Z
PKS 2053-201	2053-201	0.156	...	...	26.29	23.79	<33.49	I	-1.68	C
PKS 2058-282	2058-282	0.038	-23.25	0.74	25.67	23.69	33.46	Ig	-1.49	C,S,MT,N
PKS 2058-135	2058-135	0.046	...	...	24.89	<20.98	...	Ig	<-3.11	C
PKS 2104-256s	2104-256	0.039	...	...	25.30	22.94	...	I	...	C
3C 427.1	2104+76	0.572	...	...	28.17	24.02	...		-3.33	G
PKS 2104-25	2104-25	0.037	-22.77	0.89	26.39	23.25	33.25	I	-2.00	S,C,MT
B2 2116+26	2116+26	0.016	-23.05	...	23.57	22.73	33.45	I	1.40	M,B,N
PKS 2117-269	2117-269	0.104	...	...	25.43	22.80	33.56	II	-1.92	C
3C 434	2120+15	0.322	-22.56	0.61	27.21	...	...	II	...	Z
3C 433	2121+24	0.102	-22.92	0.75	27.09	23.34	35.34	AM	-2.95	Z,G,B
3C 435.1	2126+07	0.865	...	0.87	28.54	...	35.85	H	...	MC
3C 435	2126+07	0.471	-22.65	0.87	27.90	...	36.77	II	...	Z,MC
PKS 2128-12	2128-12	0.501	...	0.67	28.21	...	...	U	...	MT
PKS 2130-538	2130-538	0.076	-23.79	...	25.99	...	...	I?	...	Z
PKS 2134-281	2134-281	0.071	...	...	25.22	21.84	32.77	I?	-2.49	C
PKS 2135-20	2135-20	0.635	...	0.63	28.22	...	...	U	...	MT
3C 436	2141+27	0.214	-22.50	0.86	27.31	24.56	35.22	II	-1.97	S,G,R
NGC 7144	2149-48	...	-22.20	...	<22.32	22.02	<32.00	I?	...	SP,GG
PKS 2152-69	2152-69	0.027	...	0.71	26.38	24.11	34.99	I	-1.49	MT

TABLE 11—*Continued*

Name (1)	IAU (2)	redshift (3)	Magnitude (4)	α (5)	P_{total} (6)	P_{core} (7)	Line-Lum (8)	FR (9)	$R=P_l/P_c$ (10)	Reference (11)
PKS 2152-218	2152-218	0.306	-21.85	1.48	27.43	...	...	U	...	Z
3C 438	2153+37	0.291	-23.28	0.88	28.04	24.67	35.17	I	-2.41	R,LRL
PKS 2159-187	2159-187	0.332	-21.72	1.33	27.20	...	...	D2	...	Z
PKS 2159-335	2159-335	0.166	...	...	26.09	21.84	...		...	C
3C 441.0	2203+29	0.707	-24.30	0.83	28.36	<25.86	36.28	H	<-1.59	MC,G
PKS 2206-237	2206-237	0.086	...	...	25.60	24.92	34.30	U	-0.01	C
3C 444	2211-17	0.153	-24.06	1.26	27.78	24.92	33.67	II	-2.03	MT,S,C
3C 442	2212+13	0.027	-22.06	0.92	25.57	21.88	33.85	I/II	-2.69	S,B,G
3C 445	2221-02	0.056	-22.18	0.85	26.24	24.10	35.45	IId	-1.41	Z,MT
PKS 2225-308	2225-308	0.055	...	...	24.90	24.92	...	I?	...	C
3C 449	2229+39	0.017	-20.89	0.58	24.93	22.72	...	I	-1.41	S,G
B2 2236+35	2236+35	0.028	...	...	24.40	22.42	...		-1.14	G
PKS 2236-176	2236-176	0.075	...	...	25.38	24.92	33.18	I?	...	C
3C 452	2243+39	0.081	-22.63	0.78	26.93	24.56	34.72	I/II	-1.36	Z,LRL,G,R
4C 11.71	2247+11	0.023	-23.17	...	25.21	...	...	I	...	LRL
PKS 2250-41	2250-41	0.310	...	0.99	27.92	<24.22	35.98	II?	<-2.63	MT
3C 455	2252+12	0.033	-22.58	...	...	...	...	II	...	SKW
IC 1459	2254-36	...	-22.80	...	22.94	23.72	33.69	I?	...	GGX
PKS 2300-189	2300-189	0.129	-22.55	...	26.68	...	...	II?	...	Z
3C 456	2309+09	0.233	-21.81	0.40	27.34	...	...		...	SKW
3C 457	2309+18	0.428	-22.18	1.01	27.82	...	...	II	...	Z
3C 458.0	2310+05	0.290	...	0.76	27.54	...	36.02		...	MC
3C 459	2314+03	0.220	-23.18	0.74	27.53	26.46	35.44	II	0.75	Z,MT
PKS 2317-277	2317-277	0.174	...	...	26.44	23.31	34.71	IIg	-2.37	C
3C 460.0	2318+23	0.268	-22.90	0.80	27.20	<24.75	35.12		<-1.57	MC,G
PKS 2322-123	2322-123	0.082	-23.21	...	25.89	23.31	34.81	I	-3.18	Z,C
4C 27.51	2322+22	0.319	-21.74	0.89	27.03	...	...	D	...	Z
PKS 2331-240	2331-240	0.047	...	...	24.80	23.31	...		...	C
3C 465	2335+26	0.030	...	...	25.89	24.02	...	I	-1.02	G
3C 465n2	2335+26	0.029	-22.35	0.75	25.88	...	...	I	...	SKW
3C 465n1	2335+26	0.029	-23.10	0.75	25.88	...	...	I	...	SKW
3C 469.1	2352+79	1.336	-26.40	0.78	29.01	25.66	36.80	H	-2.50	MC,G
PKS 2356-61	2356-61	0.096	...	1.36	27.79	24.20	35.26	II	-2.11	MT
3C 470.0	2356+43	1.653	...	...	28.79	<26.46	...		<-1.50	G

[a] All values were derived using $H_0 = 50\ \mathrm{km\ s^{-1}\ Mpc^{-1}}$ and $q_0 = 0.0$.

Key to columns follows:
Col. (1).—Galaxy name.
Col. (2).—Redshift.
Col. (3).—Rest frame V magnitude.
Col. (4).—Spectral index (for comments see § 3.1.2), defined by $S_\nu \propto \nu^{-\alpha}$.
Col. (5).—Logarithm of the total radio power measured at 408 MHz in W Hz^{-1} (for transformations to 408 MHz, see § 2.2).
Col. (6).—Logarithm of the radio core powers measured at 5 GHz in W Hz^{-1}.
Col. (7).—Logarithm of the emission-line luminosity in watts. All measurements were converted to Hα + [N II] line luminosities as outlined in § 2.1.
Col. (8).—The FR identifications: " " = blank, FR morphology unknown, or disagreements exist in the literature; I = FR I; II = FR II; I? = most likely an FR I source; Ig = reclassified from Caganoff's sample as an unambiguous FR I; II? = most likely an FR II source; IIg = Longair & Riley's refinement to the FR II classification scheme; IIn = Longair & Riley's refinement to the FR II classification scheme; IId = Longair & Riley's refinement to the FR II classification scheme; T = transition sources; I/II = disagreements over the FR type exist in the literature; CH = core halo source (after Morganti et al. 1993); CJ = core jet source (after Morganti et al. 1993); H = high-redshift source with $z > 0.5$; U = unresolved source; C = compact source; D = double-lobed structure, but any FR classification is uncertain.
Col. (9).—Logarithm of the R-parameter (for calculations and comments, see § 3.2.2).
Col. (10).—References: col (10) gives the data source. In most cases data are simple means of the listed references unless one measurement is totally different from the others. For a more detailed explanation, see § 2.6. B = Baum & Heckman 1989a, b; BRE = Benn et al. 1993, Rowan-Robinson et al. 1993, elliptical galaxies only; C = Caganoff 1988; G = Giovannini et al. 1988; GG = Goudfrooij et al. 1993, 1994; HL = Hill & Lilly 1991; LRL = Laing et al. 1983; MC = McCarthy 1988; M = Morganti et al. 1992; MT = Morganti et al. 1993, Tadhunter et al. 1993; N = some information obtained via NED; R = Rawlings et al 1989 or Saunders et al. 1989; S = Smith 1988; SKW = Sandage 1972a, b, 1973a, b or Sandage, Kristian, & Westphal 1976 = SKW; SP = Sadler et al. 1989, Phillips et al. 1986; Z = Allington-Smith et al. 1993, or Zirbel 1993.

REFERENCES

Allington-Smith, J. A., Ellis, R. S., Zirbel, E. L., & Oemler, A. 1993, ApJ, 404, 521

Auriemma, C., Perola, G. C., Ekers, R., Fanti, R., Lari, C., Jaffe, W. J., & Ulrich, M.-H. 1977, A&A, 56, 41

Baars, J. W. M., Genzel, R., Pauliny-Toth, I. I. K., & Witzel, A. 1977, A&A, 61, 99

Baum, S. A., & Heckman, T. 1989a, ApJ, 336, 681

———. 1989b, ApJ, 336, 702

Baum, S. A., Heckman, T., Bridle, A., van Breugel, W., & Miley G. 1988, ApJS, 68, 643

Baum, S. A., Heckman, T., & van Breugel, W. 1992, ApJ, 389, 208

Baum, S. A., Zirbel, E. L., & O'Dea, P. 1995, ApJ, in press (Paper II)

Benn, C. R., Rowan-Robinson, M., McMahon, R. C., Broadhurst, T. J., & Lawrence. A. 1993, MNRAS, 263, 98

Bridle, A. H. 1992, in Extragalactic Radio Sources: From Beams to Jets, ed. J. Roland, H. Sol, & G. Pelletier (Cambridge: Cambridge Univ. Press), 386

Bridle, A. H., & Perley, R. A. 1984, ARA&A, 22, 319

Browne, I. W. A. 1983, MNRAS, 204, 23

Buson, L. M., et al. 1993, A&A, 280, 409

Caganoff, S. 1988, Ph.D. thesis, The Australian National University

Capetti, A., Parma, P., & Fanti, R. 1994, A&A, submitted

Chambers, K. C., Miley, G. K., & van Breugel, W. J. M. 1987, Nature, 329, 609

Cohen, R. D., & Osterbrock, D. E. 1981, ApJ, 243, 81

Colla, G., Fanti, C., Fanti, R., Gioia, I., & Lari, C. 1975, A&A, 38, 209

Crawford, C. S., Fabian, A. C., & Johnstone, R. M. 1987, MNRAS, 235, 183
Daly, R. A. 1992, ApJ, 399, 426
De Ruiter, H. R., Parma, P., Fanti, C., & Fanti, R. 1990, A&A, 227, 351
Fabbiano, G., Miller, L., Trinchieri, G., Longair, M., & Elvis, M. 1984, ApJ, 277, 115
Fanaroff, B. L., & Riley, J. M. 1974, MNRAS, 167, 31
Fanti, C., Fanti, R., de Ruiter, H. R., & Parma, P. 1987, A&AS, 69, 57
Feigelson, E., Isobe, T., & LaValley, M. 1992, Dept. Astron. & Astrophys. Pennsylvania State Univ. Pub. ASURV
Ferreti, L., Gioannini, G., Gregorini, L., Parma, P., & Zamorani, G. 1984, A&A, 139, 55
Giovannini, G., Ferriti, L., Gregorini, L., & Parma, P. 1988, A&A, 199, 73
Goudfrooij, P., Hansen, L., Jorgensen, H. E., & Norgaard-Nielsen, H. U. 1994, A&A, preprint
Goudfrooij, P., Hansen, L., Jorgensen, H. E., Norgaard-Nielsen, H. U., de Jong, T., & van den Hoek, L. B. 1993, A&A, preprint
Heckman, T. M., Baum, S. A., van Breugel, W. J. M., & McCarthy, P. 1989, ApJ, 338, 48
Heckman, T. M., O'Dea, P., Baum, S. A., & Laurikainen, E. 1994, ApJ, submitted
Heckman, T. M., Smith, E. P., Baum, S. A., van Breugel, W. J. M., Miley, G. K., Illingworth, G. D., Bothun, G. D., & Balick, B. 1986, ApJ, 311, 526
Hill, G., & Lilly, S. J. 1991, ApJ, 367, 1
Jackson, N., & Browne, I. W. A. 1991, MNRAS, 250, 422
Johnstone, R. M., Fabian, A. C., & Nulsen, P. E. J. 1987, MNRAS, 224, 75
Koski, A. T. 1978, ApJ, 223, 56
Laing, R. A. 1993, in Astrophysical Jets, ed. D. Burgallera, M. Livio, & C. P. O'Dea (Cambridge: Cambridge Univ. Press), 95
Laing, R. A., Riley, J. M., & Longair, M. S. 1983, MNRAS, 204, 151
Longair, M. S., & Riley, J. M. 1979, MNRAS, 188, 624
McCarthy, P. J. 1988, Ph.D. thesis, University of California at Berkeley
———. 1993, ARA&A, 31, 639
McCarthy, P. J., van Breugel, W. J. M., Spinrad, H., & Djorgovski, S. G. 1987, ApJ, 321, L29
Meier, D. L., Ulrich, M.-H., Fanti, R., Gioia, I., & Lari, C. 1979, ApJ, 229, 25
Morganti, R., Killeen, N. E. B., & Tadhunter, C. N. 1993, MNRAS, 263, 1023
Morganti, R., Ulrich, M.-H., & Tadhunter, C. N. 1992, MNRAS, 254, 546
Orr, M. J. L., & Browne, I. W. A. 1992, MNRAS, 200, 1067
Owen, F. N., & Laing, R. A. 1989, MNRAS, 238, 357
Owen, F. N., Ledlow, M. J., & Keel, W. C. 1994, ApJ, submitted
Owen, F. N., & White, R. A. 1991, MNRAS, 249, 164
Padovani, P., & Urry, C. M. 1992, ApJ, 387, 449
Phillips, M. M., Jenkins, C. R., Dopita, M. A., Sadler, E. M., & Binette, L. 1986, AJ, 91, 1061
Press, W. H., Teukolsky, S. A., Vetterling, W. T., & Flannery, B. P. 1992, Numerical Recipes (2d ed; Cambridge: Cambridge Univ. Press)
Prestage, P. M., & Peacock, J. A. 1988, MNRAS, 230, 131
Rawlings, S., & Saunders, R. 1992, Nature, 349, 138
Rawlings, S., Saunders, R., Eales, S. A., & Mackay, C. D. 1989, MNRAS, 240, 701
Rowan-Robinson, M., Benn, C. R., Lawrence, A., McMahon, R. G., & Broadhurst, T. J. 1993, MNRAS, 263, 123
Sadler, E. M., Jenkins, C. R., & Kotanyi, C. G. 1989, MNRAS, 240, 591
Sandage, A. 1972a, ApJ, 178, 1
———. 1972b, ApJ, 178, 25
———. 1973a, ApJ, 183, 711
———. 1973b, ApJ, 183, 743
Sandage, A., Kristian, J., & Westphal, J. A. 1976, ApJ, 205, 688
Saunders, R., Baldwin, J. E., Rawlings, S., Warner, P. J., & Miller, L. 1989, MNRAS, 238, 777
Shields, J. C. 1991, AJ, 102, 1314
Smith, E. P. 1988, Ph.D. thesis, Univ. of Maryland
Smith, E. P., & Heckman, T. M. 1989, ApJS, 69, 365,
Smith, E. P., Heckman, T. M., & Illingworth, G. 1990, ApJ, 356, 399
Spinrad, H., Djorgovski, S., Mair, J., Aguilar, L. 1985, PASP, 97, 932
Tadhunter, C. N., Morganti, R., di Serego Alighieri, S., Foebury, R. A. E., & Danzinger, I. J. 1993, MNRAS, 263, 999
Trinchieri, G., & di Serego Alighieri, S. 1991, AJ, 101, 1647
Urry, C. M., & Padovani, P. 1991, ApJ, 371, 60
Urry, C. M., Padovani, P., & Stickel, M. 1991, ApJ, 382, 501
Yates, M. G., Miller, L., & Peacock, A. 1989, MNRAS, 240, L129
Zirbel, E. L. 1993, Ph.D. thesis, Yale University
Zirbel, E. L. 1995a, ApJ, submitted
———. 1995b, ApJ, submitted